# Advances in mechanical detection of magnetic resonance

Seppe Kuehn,[1,a)] Steven A. Hickman,[1] and John A. Marohn[1,2,b)]
[1]*Department of Chemistry and Chemical Biology, Cornell University, Ithaca, New York 14853, USA*
[2]*Kavli Institute at Cornell for Nanoscale Science, Cornell University, Ithaca, New York 14853, USA*

(Received 6 November 2007; accepted 19 December 2007; published online 6 February 2008)

The invention and initial demonstration of magnetic resonance force microscopy (MRFM) in the early 1990s launched a renaissance of mechanical approaches to detecting magnetic resonance. This article reviews progress made in MRFM in the last decade, including the demonstration of scanned probe detection of magnetic resonance (electron spin resonance, ferromagnetic resonance, and nuclear magnetic resonance) and the mechanical detection of electron spin resonance from a single spin. Force and force-gradient approaches to mechanical detection are reviewed and recent related work using attonewton sensitivity cantilevers to probe minute fluctuating electric fields near surfaces is discussed. Given recent progress, pushing MRFM to single proton sensitivity remains an exciting possibility. We will survey some practical and fundamental issues that must be resolved to meet this challenge. © *2008 American Institute of Physics*. [DOI: 10.1063/1.2834737]

## I. INTRODUCTION

Since its discovery, nuclear magnetic resonance (NMR) has become a mainstay of fundamental physics, analytical chemistry, and structural biology by enabling the elucidation of the atomic structure of matter. While NMR has become a rich and complex spectroscopic method for probing a wide variety of materials, the possibilities that magnetic resonance offers for determining how atoms arrange themselves continues to be explored.

Here, we review approaches to expanding the sensitivity and applicability of magnetic resonance by detecting spin magnetization not inductively, as is conventionally done, but mechanically, as a force, force gradient, or torque. These methods grew out of Sidles' 1991 proposal to detect and image magnetic resonance from individual nuclei by "magnetic resonance force microscopy" (MRFM).[1,2]

In 1995, Sidles *et al.* reviewed early progress in MRFM.[3] Their paper surveyed alternative general technologies for detecting small numbers of electron and nuclear spins, summarized general design rules for pushing MRFM to single-spin sensitivity, and argued that the pressing need for new tools capable of determining the structure of a single copy of a biomolecule justified a significant investment in magnetic resonance force microscopy. The purpose of this article is to survey progress in MRFM since that landmark review.

The paper is organized as follows. In Sec. II we survey advances in competing technologies and summarize the case for continued investment in magnetic resonance force microscopy. In Sec. III we summarize nearly a decade of progress in MRFM. The 2004 milestone demonstration of single-electron magnetic resonance is discussed in some detail in Sec. IV. Our efforts to detect magnetic resonance using force gradients and to probe electric field fluctuations using ultrasensitive cantilevers are summarized in Secs. V and VI, respectively. Future directions are outlined in Sec. VII.

## II. MOTIVATION

Much of the existing detailed information about how biological systems work on a molecular level comes from knowledge of the angstrom-scale structure of the relevant molecular architectures. Such detailed information is fundamental to understanding the mechanisms of the vast array of interactions occurring between macromolecules in biological systems and is required to develop drugs that exhibit specific interactions with proteins and nucleic acids.

Before discussing recent advances in mechanically detected magnetic resonance, we present a brief overview of the most common existing techniques for determining atomic structure: x-ray crystallography and NMR. In spite of the success of these two methods, we must remember the empirical fact that the majority of proteins are not well suited for analysis by current methods because they cannot be isolated in large enough quantities or do not form crystals. A tool for determining the three dimensional structure of a single protein, such as MRFM, would indeed be a major advance.

### A. X-ray crystallography and NMR

A total of more than 35 000 protein structures have been determined by x-ray crystallography. These structures comprise more than 1000 distinct folds of proteins in more than 1200 superfamilies.[4] The central challenge for crystallographers is coaxing biological molecules to form ordered solids amenable to x-ray analysis. In addition, many important protein topologies are poorly suited to x-ray analysis. For example, transmembrane proteins are often comprised of distinct hydrophilic domains which are presented to the cytoplasm and extracellular environment and hydrophobic domains which reside in the lipid bilayer. As a result, ex-

[a)]Current address: Rockefeller University.
[b)]Electronic mail: jam99@cornell.edu.

 

pressing these proteins in high concentration often results in aggregation. Of the tens of thousands of known structures fewer than 250 are transmembrane proteins.[5]

Of the 41 000 known protein structures, more than 6000 have been determined by nuclear magnetic resonance. NMR of biological molecules is a rich field; dramatic advances have included Fourier-transform (FT) spectroscopy, nuclear Overhauser effect distance measurements, and innumerable multidimensional experiments.[6] Still, elucidating a protein structure by liquids NMR places restrictions on the structures that can be studied. As with crystallography, NMR requires expressible proteins that are soluble in millimolar concentrations. Additionally, proteins bigger than about 50 kDa become difficult to study.

Solid-state NMR (ssNMR) can in principle provide detailed structural information, especially since long-range dipolar spin-spin couplings are retained, but obtaining spectra at high resolution remains challenging.[7] Recent advances have allowed measurements on fully protonated proteins at high resolution[8] and chemical shift tensors for bond angle assignments.[9] Interestingly, ssNMR has provided the only detailed structures of amorphous amyloid fibrils important in the study of Alzheimer's disease.[10] Despite these advances, and the many important structures which have been determined, ssNMR remains limited to the study of macromolecular biomolecules that form solids and by the intrinsic low sensitivity of inductive detection.

### B. Improving NMR sensitivity

The distinct advantage of MRFM is the dramatic improvement in sensitivity over conventional inductive detection. While inductive detection, thus far, requires $\sim 10^{13}$ nuclei/$\sqrt{\text{Hz}}$ to detect an observable signal,[11,12] MRFM presents the real possibility of single nucleus sensitivity. In order to put MRFM into perspective, we briefly consider competing techniques for detecting magnetic resonance from single spins. Early high sensitivity techniques, including beam measurements, optical detection, and detection by perturbed angular correlations of radioactive nuclei emissions, have been reviewed by Abragam.[13]

Recent experiments have demonstrated the detection of magnetic resonance using a scanning tunneling microscope (STM). Manassen *et al.* have shown that electron spin resonance (ESR) can be detected as a radiofrequency oscillation in the electron tunneling current of a STM.[14–17] While the mechanism of the effect is not well understood, ESR-STM is close to demonstrating single-spin detection. However, the method requires the unpaired electron spin to be within an atomic layer of the surface, and requires a sample or sample substrate that is nearly atomically flat and either conducting or semiconducting. It is hard to see how ESR-STM could be applied to determine the angstrom-scale structure of biological samples.

In strongly luminescent materials, magnetic resonance has been detected optically with high sensitivity.[13,18–26] Although single-spin NMR and ESR optical magnetic resonance has been demonstrated in isolated molecules in doped molecular crystals at 1.2 K,[20,21,26] and at single defect sites in diamond up to room temperature,[25,27–33] these techniques lack generality and are not applicable to arbitrary organic samples. While very sensitive, optical detection lacks the spatial resolution needed for single-spin imaging where spins are a few angstroms apart as is the case in biomolecules.

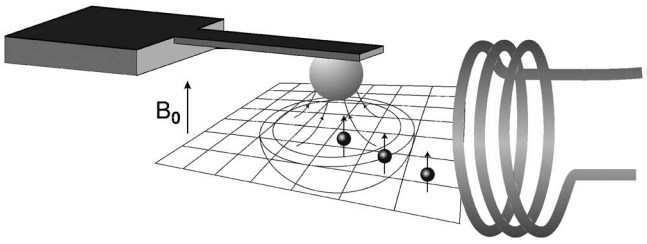


FIG. 1. A schematic of a magnet-on-cantilever magnetic resonance force microscope experiment.

Superconducting quantum interference devices (SQUIDs) are capable of detecting extremely small magnetic fluxes and have been used to detect magnetic resonance. The highest sensitivity achieved with a SQUID, to our knowledge, is 40 electron spins/ $\sqrt{\text{Hz}}$ with a $3\times 3$ $\mu\text{m}^2$ device.[34] The authors report that if they were operating this device at the theoretical thermal limit[35] at 8 K, their sensitivity would be 2.5 electron spins/ $\sqrt{\text{Hz}}$. While SQUID detection exhibits exquisite sensitivity and is generally applicable to nuclear and electron magnetic moments, like optical detection it lacks sufficient spatial resolution to elucidate detailed atomic connectivity.

These single-spin detection techniques cannot generally be applied to detect NMR in large biomolecules in the condensed phase. In contrast, MRFM puts few restrictions on the properties of the sample that can be studied and no restrictions on the type of magnetic moment that can be interrogated. Magnetic resonance force microscopy remains the most feasible route yet proposed for detecting single-spin NMR in large biomolecules at high sensitivity and high spatial resolution.

## III. RECENT ADVANCES IN MECHANICALLY DETECTED MAGNETIC RESONANCE

A schematic of early MRFM experiments appears in Fig. 1. A magnetic-tipped cantilever is brought close to a sample surface containing spins to be studied. The spins can be unpaired electron spins or nuclear spins, e.g., hydrogen nuclei. A polarizing magnetic field $B_0$ may be applied to align the sample spins. A radio frequency (rf) magnetic field produced by a nearby coil is applied to the sample. The rf is resonant with spins in a constant-field "sensitive slice" in which the magnetic field induced spin energy level splitting equals the energy of the rf radiation. The rf frequency (or the polarizing field) is modulated so that the spins in the sensitive slice are cyclically inverted at the cantilever's mechanical resonance frequency, a few kilohertz typically. Through the gradient-dipole force between the sample spins and the magnetic particle at the end of the cantilever, the cyclic spin inversion drives the cantilever into an oscillation of a few nanometers amplitude. The cantilever oscillation is detected with an optical fiber interferometer (not shown).

The MRFM experiment works equally well with the sample affixed to the cantilever. All early experiments were performed this way for convenience. A flurry of activity followed the initial demonstration that microcantilevers could be used to detect electron spin resonance[36] and nuclear magnetic resonance.[37] The purpose of this section is to detail key experiments and ideas in magnetic resonance force microscopy that have been developed since the comprehensive review of Ref. 3.

### A. Sensitivity

The magnetic moment sensitivity of the MRFM experiment sketched in Fig. 1 is given by $\mu_{\min}=F_{\min}/G$, where $F_{\min}$ is the oscillator's minimum detectable force and $G$ is the magnetic field gradient arising from the cantilever tip, acting on the target spin. The oscillator's minimum detectable force depends on the detection bandwidth $b$ and on the spectral density $S_F$ of stochastic thermal forces acting on the cantilever: $F_{\min}=\sqrt{S_F b}$. This spectral density is related, via the fluctuation-dissipation theorem, to the friction experienced by the oscillator: $S_F=4\Gamma_t k_B T$, where $\Gamma_t$ is the total friction experienced by the oscillator, $k_B$ is Boltzmann's constant, and $T$ is temperature. Thus,

$$\mu_{\min}=\frac{1}{G}\sqrt{4\Gamma_t k_B T b}. \tag{1}$$

Equation (1) indicates that improving magnetic moment sensitivity demands minimizing all sources of cantilever friction, carrying out experiments at low temperature, and employing small magnetic particles to produce large gradients. Advances in MRFM sensitivity have followed from improvements in all of these areas.

A commercially available silicon nitride cantilever was used in the first demonstration of mechanically detected ESR.[36] To improve sensitivity, a custom-fabricated, low spring constant, 90-nm-thick silicon nitride cantilever with a record low intrinsic friction was harnessed in the first demonstration of mechanically detected NMR.[37] These experiments inspired the development of cantilevers with vastly improved sensitivity.

By fabricating single-crystal silicon cantilevers having spring constants of only 6.5 $\mu$N/m, Stowe *et al.* obtained an unprecedented force sensitivity of $\sqrt{S_F}=5.8$ aN/$\sqrt{\text{Hz}}$ at liquid helium temperatures in vacuum.[38] Initial experiments also demonstrated that these extremely compliant cantilevers could be brought within 10 nm of a surface without snapping in to contact as long as their motion was parallel with the surface of the sample. Such attonewton-sensitive cantilevers, a thousand times more compliant than the best commercially available cantilevers, have now been fabricated by a number of groups for use in MRFM experiments.[39–43]

While MRFM can be carried out at ambient pressure and temperature,[44,45] nearly all experiments to date have been performed in vacuum to reduce cantilever friction which is high in air, and to facilitate working at cryogenic temperatures. Improved sensitivity at cryogenic temperatures was first demonstrated in the NMR-MRFM experiment of Wago *et al.* in which a Nd-doped sample of $CaF_2$ was affixed to a commercial silicon cantilever.[46] MRFM measurements at the highest levels of sensitivity have been carried out at 4 K and below.

Early experiments employed gradients of 300–2200 T/m produced by a 100 $\mu$m scale magnetic shard.[47] Even the first demonstration of "magnet on tip" MRFM, though a remarkable development, employed a large enough magnetic tip that the gradient was not much larger than in early experiments.[48] By gluing magnets as small as 5 $\mu$m to commercial silicon nitride cantilevers and operating the cantilevers within a few tens of nanometers of a surface, Bruland *et al.*[49] were able to detect electron spin resonance using magnetic field gradients as large as $2.5\times10^5$ T/m. The sensitive slice in these experiments was only a nanometer thick, on the order of molecular dimensions. Remarkably, at a temperature of 77 K, Bruland *et al.* achieved a magnetic moment sensitivity of $\sim 200\mu_e/\sqrt{\text{Hz}}$. Most recent high sensitivity MRFM measurements have been made with gradients $\geqslant 10^5$ T/m; the largest gradient employed to date is $1.4\times10^6$ T/m.[50]

### B. Spurious response evasion, cantilever control, and instrumentation

Cantilever response is largest when the force acting on the cantilever is applied coherently at the cantilever's resonance frequency $f_c$. Depending on the sample's spin lattice relaxation time, modulating the force in early MRFM experiments was accomplished by either periodically saturating the sample magnetization via amplitude modulating the applied rf (when $T_1<f_c^{-1}$) (Ref. 36) or by performing cyclic adiabatic rapid passages via sweeping the frequency of the applied rf or the static magnetic field (when $T_{1\rho}>f_c^{-1}$.[37] In order to avoid the spurious response of the cantilever to the modulated rf, a number of alternative schemes of modulating magnetization were developed. These schemes employed joint anharmonic modulation of rf frequency and field (either electronically[51] or mechanically[52]) and parametric amplification of the spin signal.[53]

The natural response time of the most force sensitive cantilevers is usually much longer than the coherence time of the spin being detected. As in atomic force microscopy, feedback can be used to shorten the time required for the cantilever's amplitude to reach steady state in response to a resonant force.[37,54] Optimal control theory has been applied to design high-performance MRFM cantilever controllers,[55] implemented at audio frequency using analog[56] and digital electronics[57–60] and at radio frequency using digital heterodyning downconversion in conjunction with a field programmable gate array.[61]

Another approach to mitigating the slow natural response time of a cantilever is to detect the spins mechanically using force gradients instead of forces. In principle, a force gradient shifts the cantilever frequency instantaneously. In practice, such shifts can indeed be detected very rapidly by measuring the cantilever frequency while the cantilever is driven into self-oscillation using positive feedback.[62] Two force-gradient approaches to detecting magnetic resonance will be discussed in detail below, in Secs. IV and V.

In addition to spurious response evasion and cantilever control, early experiments benefited from developments in rf coil design,[63] microscope design,[64–66] and digital rf generation.[67] An advance that simplified microscope design considerably was the demonstration that the optical interferometer ubiquitously used to detect cantilever motion in MRFM experiments could be tuned on fringe by adjusting the temperature of the interferometer's laser, external to the MRFM probe.[68]

### C. Imaging

The first electron-spin resonance MRFM experiment produced a one dimensional image by scanning the magnetic field to sweep the sensitive slice through the sample. Two and three dimensional unpaired-electron-density images of phantom samples were soon obtained by adding lateral scanning;[69–71] spin density images were obtained via deconvolution of the resulting force map. The dependence of the ESR-MRFM signal line shape on rf field strength and static field (or rf frequency) modulation has now been modeled in detail.[72,73]

In an exciting first step towards a biological application, a nitroxide-labeled liposome membrane was prepared and imaged by MRFM.[74] Resolution in three dimensional (3D) ESR imaging experiments has been pushed to nanometer scale by working with gradient sources as small as 5 $\mu$m mounted to a commercial silicon nitride cantilever.[75] Many of these experiments required long imaging times, achieved with careful closed-loop control of scanning;[76,77] acquisition times as long as ten days have been demonstrated in a 3D ESR imaging experiment.[76]

Three dimensional imaging was extended, early on, to include nuclear magnetic resonance, by scanning the field and sample,[47] again using a deconvolution of the force map to construct an image. A one dimensional image in GaAs was demonstrated with 170 nm resolution[78] in an experiment in which the GaAs was optically pumped with circularly polarized light to increase nuclear spin polarization. More recently, Mamin and coworkers achieved a record 90 nm resolution in a two-dimensional imaging experiment detecting magnetization fluctuations in a patterned $CaF_2$ sample.[50] Eberhardt *et al.* have shown that a substantial improvement in image acquisition time can be obtained by acquiring signal simultaneously from multiple slices whose magnetization has been premodulated in a Hadamard pattern.[79] Note that the sample was attached to the cantilever in the experiments of Refs. 78, 50, and 79.

Other imaging protocols have been considered. If the magnetic particle gradient is sufficiently large, it has been predicted that distinct peaks should be observable in the MRFM signal, as the sample is scanned through the sensitive slice or as the field is rotated. These peaks contain information on the lattice spacing.[80–83] Another proposed approach to imaging is to use a magnetic lens to confine resonance to a sensitive point, which is then scanned.[84]

Unless the sample is inherently planar, observing a selected plane in the sample using the imaging protocols demonstrated in Ref. 47 (or proposed in Refs. 80–83) requires collecting and reconstructing an entire 3D image of the sample. This procedure might be extremely time consuming; at 1 s per point, acquiring an image with $64^3$ pixels requires three days of signal acquisition. The imaging protocol proposed in Ref. 84 might only require, for example, acquiring $64^2$ data points to produce planar image, but, by analogy with conventional magnetic resonance imaging, most certainly at the expense of signal to noise per unit time.[85]

In conventional magnetic resonance imaging high-sensitivity planar images are formed by exciting spins in a sensitive slice and then Fourier encoding the lateral position of the spins using time-switched magnetic field gradients. It has been proposed that Fourier image encoding can be achieved in a MRFM experiment by laterally shuttling (in $x$ and $y$) the cantilever's magnetic tip in synchrony with an rf pulse sequence.[86] In this approach, Fourier transforming the spin signal as a function of the two shuttling times (or amplitudes) should reveal a two dimensional "spectrum" whose lines are distributed according to resonance shifts proportional to each spin's $(x,y)$ location in the sensitive slice. Note that these shifts, in contrast to all previous magnetic resonance imaging approaches,[87,88] are proportional to the gradient, not the field, at each pixel.

This FT-MRFM scheme has a number of potential advantages over demonstrated MRFM imaging approaches.[47] It replaces a sensitivity-degrading nonlinear 3D signal deconvolution with a sensitivity-preserving linear two dimensional Fourier transform. It requires only small nanometer-scale motions of the tip, whereas 3D deconvolution requires scanning over an area much larger than the sample. In FT-MRFM, the $x$, $y$, and $z$ pixel sizes may be varied independently according to the amplitudes of the shuttle motions and the thickness of the region of detected spins. Projections of spin density onto arbitrary planes can be collected by shuttling along a linear combination of $x$ and $y$ directions. In the single-spin limit, these projection signals could greatly decrease the number of experiments required to obtain a 3D molecular image, by using Kupce and Freeman's algorithms for reconstructing a spectrum from just a few time-domain experiments.[89,90] While the FT-MRFM pulse sequence examined in Ref. 86 might have too high a duty cycle to avoid cantilever heating in an MRFM experiment, the approach of Ref. 86 can be applied with far simpler pulse sequences such as a stimulated echo.

### D. Ferromagnetic resonance and other applications

One promising application of magnetic resonance force microscopy is detecting ferromagnetic resonance (FMR). Ferromagnetic resonances are collective spin-wave oscillations of the strongly coupled electron spins in a magnetic material and are an exquisitely informative probe of the magnetism of thin films and nanostructures. Ferromagnetic resonance frequencies are determined by the details of the spin-spin coupling as well as by the shape of the sample and the static magnetic field; ferromagnetic spectra can be very challenging to simulate.

Ferromagnetic resonance can be registered as either a force[48,91–104] or a torque[105] acting on a cantilever. New infor-

mation about magnetic damping can be obtained by combining microwave susceptibility measurements, which probe transverse magnetization, with MRFM measurements, which probe longitudinal magnetization.[94,96–98,100] The influence of the magnetic tip on the ferromagnetic resonances in these experiments has required careful analysis.[48,95,104,106] Variable-temperature ferromagnetic resonance measurements have recently been demonstrated.[107]

Other potential applications of magnetic resonance force microscopy that have been explored experimentally include magnetic field mapping using ESR (Ref. 108) and FMR,[109] examining spin injection in spintronics devices,[110] and exciting electron spin in an atomic vapor for cold-atom metrology applications.[111] Using a magnetic resonance force microscope to implement a quantum computer has been proposed and investigated theoretically.[112–114]

### E. Spectroscopy

The first cryogenic NMR-MRFM experiment measured the spin-lattice relaxation time of the sample.[46] In another early experiment by Wago *et al.*, it was shown that magnetic resonance force microscopy could observe the ESR line splitting arising from hyperfine coupling of donor electrons to the $^{31}$P donor nuclear spin in silicon.[115] The promise of spectroscopic measurements continued with a demonstration of MRFM-detected nutation and spin echoes.[116] Nutation spectroscopy was extended to quadrupolar nuclei in an experiment detecting NMR from five nuclei using MRFM ($^{23}$Na, $^{69}$Ga, $^{71}$Ga, $^{27}$Al, and $^{51}$V).[117]

More recently, MRFM has been used to carry out spin echo spectroscopy[118] and observe dipolar spin echoes[119] in solids. Cross polarization[120] and indirect observation of low gamma nuclei via cross depolarization[121] have now also been demonstrated in an MRFM experiment. This work suggests that cross polarization is a possible route to obtaining image contrast in MRFM.

A consideration of the broadening effect of the gradient on the magnetic resonance signal makes it clear that these MRFM spectroscopy experiments rely to some extent on having relatively weak gradients (as well as very strong transverse rf fields). Leskowitz and co-workers proposed[122] and built[123] an apparatus to mechanically detect magnetic resonance that, remarkably, avoids this seemingly necessary compromise. Their approach involves manufacturing a homogeneous field using compensated gradient magnets, only one of which is attached to the cantilever. This innovation allowed force detection, for the first time, of nuclear magnetic resonance from a liquid and, simultaneously, observation of an indirect $J$ coupling by force detection.

### F. New spin physics

An early theoretical examination of single-spin detection by mechanical and electrical means was made in Ref. 124, which investigated whether the magnetization of a single spin would remain well behaved enough during irradiation and readout when coupled strongly to a radio frequency cantilever. MRFM experiments to date have avoided the potential pathologies uncovered in this paper by detecting longitudinal magnetization using audio frequency cantilevers.

Force-detected ESR experiments on diphenyl picrylhydrazyl-doped polystyrene carried out in a gradient of $4.4\times10^4$ T/m and at 10 and 77 K uncovered two anomalous behaviors: the electron $T_1$ (inferred from the signal's phase lag) was shorter than expected and the force signal saturated much more slowly than expected at high power.[66] A number of candidate phenomena were identified as potential causes of this anomalous behavior, including magnetization relaxation by paramagnetic defects (such as oxygen) in the film, relaxation due to tip magnetization fluctuations (from paramagnetic spins, domain wall motion, ferromagnetic spin excitations, or conduction-band thermal-magnetic noise), or spin diffusion (possibly modified by the strong gradient).

Definitive evidence that magnetization fluctuations in the tip can affect the electron spin-lattice relaxation time ($T_{1e}$) of the sample in a MRFM experiment was provided by Stipe *et al.*[125] They studied $E'$ centers in fused silica and employed a high-coercivity $Pr_2Fe_{14}B$ particle that had been milled to a diameter of 1.25 $\mu$m to produce a gradient of $1\times10^5$ T/m. They observed a decrease in $T_{1e}$ due to proximity to the tip. Comparison to theory suggested that magnetic noise from thermal currents in the tip was a more likely cause of the observed $T_{1e}$ lowering than transverse magnetization fluctuations in the tip.

Depending on the tip material and size, the tip can also increase $T_{1e}$. Budakian *et al.* studied essentially the same sample but used a somewhat larger 6.5 $\mu$m diameter tip made instead of $Sm_2Co_{17}$. In their study they varied the gradient from 10 to $3.6\times10^4$ T/m and found that the electron spin-lattice relaxation rate of the sample's $E'$ centers was lower in the biggest gradients.[126] This lowering was the result of the biggest applied gradients introducing a large enough resonance offset between adjacent $E'$ centers that flip-flop interactions were suppressed. This suppression of flip-flop interactions inhibited spin diffusion, which affected relaxation. The phenomena seen in the Budakian *et al.* experiment have been studied via numerical simulations.[127]

Striking direct evidence that a field gradient affects nuclear spin diffusion has been recently provided by Eberhardt *et al.*, who used MRFM to acquire time-resolved one dimensional images of diffusing Curie-law magnetization in $CaF_2$.[128] The observed gradient-induced decrease in $^{19}$F spin diffusion rate, and the effect of pulses on the rate, could be explained using a picture of gradient-coupled Zeeman and dipolar spin reservoirs.

These effects were observed using audio frequency cantilevers. Employing radio frequency cantilevers in a MRFM experiment could open up new possibilities for observing novel and potentially useful new spin physics.

Weitekamp has considered the consequences of coupling a spin system to a radio frequency oscillator (for example, a cantilever or a torsional oscillator).[129] If the oscillator's mechanical frequency is attuned to the Larmor frequency of the spins, then the mechanical oscillator may play the role of the electromagnetic cavity in the usual quantum electrodynamics description of spin-radiation coupling. Analogs of spontaneous emission, stimulated emission, and stimulated absorbtion

follow, in which the spin system exchanges quanta with the mechanical mode. This kind of nonunitary spin-oscillator coupling is predicted to result in an advantageously rapid spin-lattice relaxation time at low temperature. Alternatively, the coupling could allow rapid dynamic nuclear polarization of the spin system if the oscillator can be cooled by, for example, applying damping feedback.

Bargatin *et al.* have described how nuclear spins undergoing dynamic nuclear polarization (for example, via electron-nuclear coupling to an irradiated paramagnetic dopant) while coupled to a radio frequency cantilever should give rise to laserlike behavior of the spin-cantilever system.[130] Effects resulting from cantilever-induced stimulated emission of the nuclear spins ranging from "giant pulses" and ringing superradiance to full-fledged lasing have been predicted.

### G. From sample-on-cantilever to magnet-on-cantilever experiments

Applying MRFM to study technologically interesting samples demands mounting the magnetic particle on the cantilever. Zhang and Hammel first considered the possibility of performing an MRFM experiment with the magnetic particle on the cantilever. In their control experiments they found that the interaction of the magnetic tip with the field led to huge magnetic field dependent variations in the mechanical frequency of the cantilever. They concluded that the tip magnetic moment must be minimized and that the applied polarizing field must be highly uniform.[131,132]

Magnet-on-tip cantilever detection of ESR was demonstrated by Wago *et al.*[48] These experiments, though successful, indicated that operating the magnetic-tipped cantilever in high magnetic field also leads to a catastrophic increase in cantilever friction. This effect was not present in the magnet-on-cantilever ESR experiment of Bruland *et al.* because the polarizing field was zero and the tip field was used to polarize the sample.[49] In an NMR experiment, working near zero field would lead to unacceptably low Curie-law magnetization.

With an eye towards carrying out a magnet-on-cantilever NMR-MRFM experiment at high magnetic field, Marohn *et al.* showed that a large magnetic tip could, in fact, be operated at high magnetic field without loss in cantilever force sensitivity.[133] The magnetic field was aligned along the direction of the width of the cantilever; in this orientation the magnetic particle remained parallel to the magnetic field over a cantilever cycle. In this orientation, information about the tip's magnetic moment was obtained by using an applied oscillating quadrupole gradient coil. For tip magnetic moments oriented along the cantilever length, Marohn *et al.* developed and tested a model relating the tip's saturation magnetization, volume, and shape anisotropy to the observed change in cantilever frequency versus field. This opened the door to quantitative cantilever magnetometry.[40,134–136]

As ever smaller diameter tips were used in MRFM experiments, concern was voiced that thermally induced tip magnetization fluctuations might deleteriously affect sample spins.[137] Magnetization fluctuations would lead to magnetic field fluctuations at the sample spins; the spectral density of these fluctuations at the Larmor frequency could lower $T_1$, while the spectral density at the Rabi frequency could lower $T_{1\rho}$. Micromagnetic simulations indicated that, at low applied field, tips should be made of high-anisotropy materials instead of low-anisotropy materials, essentially because internal fields in the high-anisotropy materials push magnetization fluctuations to frequencies well above the electron Larmor frequency in paramagnetic samples.

The spectral density of magnetization fluctuations at a cantilever frequency (a few kilohertz) can be measured, via cantilever magnetometry, by affixing the magnet under study to a cantilever and following the change in quality factor as a function of magnetic field. Stipe *et al.* used cantilever magnetometry to show that the audio frequency thermomagnetic fluctuations were indeed much less in $Pr_2Fe_{14}B$ than in cobalt.[134] These studies motivated a switch from nickel and cobalt to rare-earth magnets such as $Sm_2Co_{17}$ and $Pr_2Fe_{14}B$ in ESR-MRFM experiments. Even so, it appeared that electron spin $T_1$ and $T_{1\rho}$ were still being shortened due to proximity of sample spins to the magnetic (metallic) tip.[125]

Another tip-related spin relaxation mechanism was identified by Mozyrsky *et al.*:[138] thermomechanical noise in the higher-order modes of the cantilever. Because of the presence of the magnetic field gradient in an MRFM experiment, any cantilever motion leads to a change in the magnetic field seen by sample spins. Since the cantilever's higher-order modes have spectral density at the electron's Rabi frequency, the random thermal motion in these modes should lead to a decreased $T_{1\rho}$. This effect was mitigated by fabricating cantilevers of nonuniform thickness having much fewer higher-order modes near the spin Rabi frequency.[139] Fabrication of such cantilevers subsequently led to improved spin relaxation rates in ESR-MRFM experiments.[140] It has been proposed that another route to minimizing tip magnetic noise is to fabricate a cantilever with a nonuniform thickness tailored to suppress the amplitude of high-frequency eigenfunctions at the position of the cantilever's magnetic particle.[141]

In preparation for performing magnet-on-cantilever NMR experiments at high field using the tip-field geometry of Ref. 133, Ng *et al.* used cantilever magnetometry to reexamine the assumption that high-anisotropy tips are the best choice for MRFM experiments.[136] Comparing magnetization fluctuations in cobalt and nickel, they reached the conclusion that using very *low* anisotropy tips and working at high magnetic field is another approach to minimizing tip field fluctuations. This approach relies on the idea that low-frequency magnetization fluctuations in the low anisotropy material are more easily damped by the applied field.

Magnet-on-cantilever mechanical detection of NMR was first demonstrated by Garner *et al.*, as described in Sec. V below.

### H. Crossing the small ensemble threshold

The most force sensitive cantilevers must be operated with their long axis perpendicular to the surface[38] to avoid snap in to contact. However, because of the symmetry of the tip's field gradient in this geometry, the net force between the cantilever's magnetic tip and a uniform plane of sample

spins is *zero*. In this case, a force on the cantilever is only observable if there exists a statistical imbalance in the number of spins to either side of the cantilever. Fortunately, as more sensitive cantilevers were developed, ever larger gradients were used, and more effective readout schemes were devised, such statistical fluctuations in electron-spin magnetization became observable by MRFM.[140]

Detecting statistical fluctuations in magnetization requires observing a small ensemble of spins. For $N$ electrons, the Curie Law magnetization is $\mu_{\text{spin}}=Np\mu_e$, where $p=\mu_e B_0/k_B T$ is the Boltzmann polarization of the spins at temperature $T$ in an applied field $B_0$. In the limit of weak polarization, $p\ll 1$, spins are distributed up or down at random and, consequently, there exists a statistical fluctuation in the magnetization having a variance of $\sigma^2_{\text{spin}}=N\mu_e^2$. When $\sqrt{N}\gg Np$, the standard deviation $\sqrt{N}\mu_e$ in the magnetization is larger than the average Curie-law magnetization. In this regime, $\sigma_{\text{spin}}/\mu_{\text{spin}}>1$, and stochastic fluctuations in the polarization which are much larger than the Curie-law polarization occur with high probability, effectively polarizing the ensemble being measured.

In the experiment of Mamin *et al.*,[140] few enough spins were observed that $\sqrt{N}\gg Np$. While statistical fluctuations in magnetization are expected to be present along the $z$ axis in the laboratory frame, Mamin *et al.* showed that statistical fluctuations in magnetization are likewise present along the direction of the effective field in the rotating frame of spins undergoing adiabatic rapid passages. These rotating-frame magnetization fluctuations showed a Lorentzian correlation function with a correlation time between $T_1$ and $T_{1\rho}$, in qualitative agreement with theory.[142]

Subsequent experiments demonstrated the manipulation of statistical fluctuations by applying pulses to rectify electron magnetization and store rotating-frame magnetization fluctuations along the laboratory $z$ axis.[143] Detection and manipulation of statistical nuclear magnetization was also demonstrated, in three different samples.[144] Building on a correlation-function approach outlined by Carson *et al.*,[145,146] Mamin *et al.* demonstrated that both transient nutations and $T_2^*$ could be measured with statistical nuclear magnetization.

The experiment of Ref. 140 was moreover an important milestone because it showed that a statistical spin polarization could be discerned, by power averaging and lock-in detection, even when the spin signal has random sign. Since the resulting insights into how to definitively detect a random-sign signal in the presence of random-sign noise are crucial to designing and implementing all subsequent high-sensitivity MRFM experiments, we will discuss them briefly here.

Let us first recall how usual signal averaging works. For signal corrupted by additive Gaussian white noise, the standard error in the mean signal after $n$ averages is improved by signal averaging to $\sigma_\mu=\sigma^2_{\text{noise}}/n$, where $\sigma_{\text{noise}}$ is the standard deviation in the noise. The familiar amplitude signal-to-noise ratio is $\text{SNR}_A=\mu_{\text{spin}}/\sigma_\mu=\sqrt{n}\mu_{\text{spin}}/\sigma_{\text{noise}}$. The ratio of signal power to noise power is

$$\text{SNR}_P=n\frac{\mu^2_{\text{spin}}}{\sigma^2_{\text{noise}}}, \tag{2}$$

and improves linearly with the number of averages.

Signal averaging a random-sign signal such as a statistical fluctuation in magnetization requires averaging the square of the signal, e.g., the signal *power*. Consider first the limiting case in which the main source of indeterminate error in the signal power is not detector noise but statistical variations in the sample's magnetization itself. In this case, if $N$ is large and $p\ll 1$, the electron magnetization will be Gaussian-distributed with a mean of zero and a variance of $\sigma^2_{\text{spin}}=N\mu_e^2$. Let $s^2_{\text{spin}}$ be the variance in magnetization inferred from $n$ measurements. From probability theory, it is known that $s^2_{\text{spin}}/\sigma^2_{\text{spin}}$ is distributed according to a $\chi^2$ distribution with $n-1$ degrees of freedom,[147] from which it follows that the standard deviation in the measured signal variance is $\sigma_{s^2_{\text{spin}}}=\sigma^2_{\text{spin}}(2/(n-1))^{1/2}$. The power signal-to-noise ratio is

$$\text{SNR}_P\approx\frac{\sigma^2_{\text{spin}}}{\sigma_{s^2_{\text{spin}}}}=\left(\frac{n-1}{2}\right)^{1/2}, \tag{3}$$

valid in the approximation that $\sigma_{\text{spin}}\gg\sigma_{\text{noise}}$. Equation (3) describes signal averaging in the absence of detector noise such as thermomechanical fluctuations in the cantilever position.

The second limiting case to consider is one where the variance in (Gaussian-distributed) instrument noise $\sigma^2_{\text{noise}}$ is much larger than the variance $\sigma^2_{\text{spin}}$ of the spin signal. Here, the spins are modulated and detected with a lock-in amplifier and the lock-in phase is set such that the spin signal is restricted to the $x$ channel, while the noise is present in both $x$ and $y$. The spin signal is inferred by subtracting variances: $s^2_{\text{signal}}=s^2_x-s^2_y$. If $\sigma_{\text{noise}}\gg\sigma_{\text{spin}}$, then after $n$ averages $\sigma^2_{s^2_x}\approx\sigma^2_{s^2_y}=(2/(n-1))\sigma^4_{\text{noise}}$.[148] Assuming that the noise in each channel is uncorrelated, the standard deviation in the variance $s^2_{\text{signal}}$ after $n$ measurements is $\sigma_{s^2_{\text{signal}}}=(2/(n-1))^{1/2}\sqrt{2}\sigma^2_{\text{noise}}$. The power signal-to-noise ratio is

$$\text{SNR}_P=\frac{\sigma^2_{\text{spin}}}{\sigma_{s^2_{\text{signal}}}}=\left(\frac{n-1}{2}\right)^{1/2}\left\{\frac{\sigma^2_{\text{spin}}}{\sqrt{2}\sigma^2_{\text{noise}}}\right\}, \tag{4}$$

valid when $\sigma_{\text{noise}}\gg\sigma_{\text{spin}}$. Again, the signal-to-noise ratio improves as the square root of the number of averages, provided that the initial signal to noise is calculated by ratioing signal power to noise power. Equation (4) describes signal averaging in the single-spin experiment of Ref. 149 discussed in Sec. IV below.

Signal averaging when $\sigma_{\text{spin}}$ and $\sigma_{\text{noise}}$ are comparable has been recently treated by Degen *et al.* who find, remarkably, that periodically rerandomizing the spin ensemble using applied rf pulses can increase SNR.[148]

## IV. THE SINGLE ELECTRON MILESTONE

MRFM detection and one-dimensional imaging of magnetic resonance from a *single* electron spin was reported in 2004 by Rugar *et al.*[149] The exceptional sensitivity demonstrated in this measurement was achieved through many of the developments detailed above, including fabrication of

attonewton-sensitive cantilevers and operation of these cantilevers in high vacuum at cryogenic temperatures to improve force sensitivity; fabrication of submicron diameter ion-beam-milled tips to increase the gradient and hence the force per spin; and the use of high-anisotropy tip magnets and special mass-loaded cantilevers to minimize extraneous magnetic field fluctuations which might disturb the target spin. In this section we summarize the key additional innovations that led to the breakthrough of single electron spin detection by MRFM.

The first set of innovations involved adapting MRFM experiments for operation at a temperature of 4 K and below. To detect cantilever motion without heating the cantilever at cryogenic temperatures, where its thermal conductivity is low, an interferometer was developed which employs only a few nanowatts of optical power.[150] To flip sample spins without unduly heating the cantilever or the sample, a superconducting microwave resonator was devised which generated a 3 GHz magnetic field of amplitude of 4 G while only dissipating 320 $\mu$W of power.[151]

The second innovation involved a low-background method for detecting and power averaging the small, random mechanical force that a single spin presents to the cantilever. Modulating spins in a MRFM experiment typically requires varying the frequency or amplitude of the applied rf. For the most sensitive magnetic-tipped cantilevers, these modulations lead to either a troublesome background driving of the cantilever or drift in its resonance frequency. In order to mechanically detect magnetic resonance from a small number of spins, it was necessary to invent a method for flipping spins that would lead to a discernible driving of the cantilever by spins yet would avoid these troublesome effects.

In the oscillating cantilever-driven adiabatic reversals (OSCAR) approach to detecting magnetic resonance introduced by Stipe *et al.*, the rf is left on continuously as the cantilever is self-oscillated via positive feedback.[125] Spins below the cantilever are swept through resonance once per cantilever cycle by the oscillating longitudinal field created by the moving magnetic tip. Viewed from the moving reference frame of the cantilever, a spin gradient in the sample is present which provides a symmetric restoring force on the cantilever. This restoring force shifts the cantilever's spring constant by an amount

$$\Delta k_z = \frac{\partial \mu}{\partial z}\frac{\partial B_z}{\partial z}, \tag{5}$$

where $\mu$ is the sample's spin magnetic moment, $B$ is the magnetic field from the tip, and $z$ is the direction of cantilever motion.[152,153] This change in the cantilever spring constant is observed as a spin-dependent shift in the resonance frequency of the cantilever.

While measurement of a cantilever's frequency is ideally thermally limited, all high-compliance cantilevers used in MRFM experiments to date experience extraneous frequency fluctuations near surfaces (as will be discussed below). Mamin *et al.* demonstrated an interrupted-OSCAR (iOSCAR) protocol[140] in which the spin-dependent shift in cantilever frequency is modulated at $f_c/m$ by turning off the rf for half a cantilever period every $m$ cycles. This modulation moves the spin signal to a frequency $f_c \pm f_c/m$, away from surface-induced $1/f$ noise centered at $f_c$ in the cantilever frequency power spectrum. In demonstrating iOSCAR, Mamin *et al.* also showed that the spring constant shift of Eq. (5) can be applied to observe small-ensemble magnetization fluctuations using a cantilever operating with its long axis perpendicular to the sample surface.

In addition to the these innovations, achieving single-spin detection required building an exceptionally stable apparatus. While the single-shot signal-to-noise in the experiment of Ref. 149 was 0.06, the apparatus was so stable that up to 12 h per data point of signal averaging could be carried out.[149] This stability enabled not only the highest magnetic moment sensitivity ever achieved, but also a record (one dimensional) magnetic resonance imaging resolution of 25 nm.

## V. A FORCE-GRADIENT APPROACH TO DETECTING NUCLEAR MAGNETIC RESONANCE

The spin-lattice relaxation time in the rotating frame, $T_{1\rho}$, limits how long spin-locked magnetization can be cyclically inverted. Both force-based and iOSCAR-based approaches to mechanically detecting magnetic resonance require samples with $T_{1\rho} \geqslant 100$ ms in order to build up a cantilever excitation large enough to detect in the presence of background thermomechanical fluctuations.[144] The success of Rugar *et al.*'s single-electron-spin experiment therefore also depended critically on identifying a sample whose electron spins could be spin locked for many hundreds of milliseconds or longer.

Previous low-temperature NMR-MRFM samples—$CaF_2$ and GaAs, for example—had also been carefully chosen, in this case to have nuclear spins with a favorable $T_{1\rho}$. In technologically and scientifically interesting samples such as organic electronic materials or biopolymers, it is highly unlikely that nuclear spins' $T_{1\rho}$ will be long enough to sensitively detect nuclear magnetic resonance using either force-based or iOSCAR based approaches at cryogenic temperatures where force sensitivity is greatest.

### A. The CERMIT experiment

To address this shortcoming in existing techniques, we developed a new method for detecting magnetic resonance. Our protocol, cantilever enabled readout of magnetization inversion transients (CERMIT), does not require that spins remain locked in the rotating frame during detection. The CERMIT effect is illustrated conceptually in Figs. 2(a) and 2(b).

The basis for the effect is a force gradient that couples a magnetic-tipped cantilever to the longitudinal component of sample magnetization, $\mu_z$. For the tip-sample geometry sketched in Fig. 2(a), each spin's contribution to the force gradient is $\mu_{zj}\partial^2 B_z(\mathbf{r}_j)/\partial x^2$. If the sample is a uniform half-space of spins, the number of spins in regions where $\partial^2 B_z/\partial x^2$ is positive and negative is roughly equal and, consequently, $\Delta k_x \approx 0$. In the CERMIT experiment, this unfortunate cancelation is remedied by applying a single adiabatic rapid passage to the sample spins. The rapid passage creates an inverted region of spins lying between two constant-$B_z$

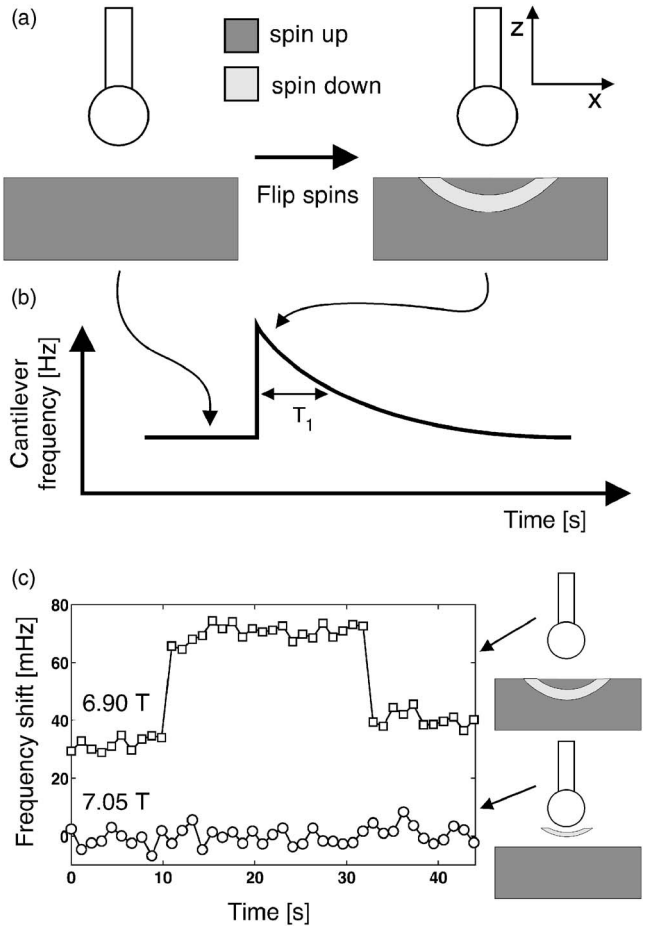


FIG. 2. The cantilever enabled readout of magnetization inversion transients, or CERMIT, approach to mechanically detecting magnetic resonance. (a) A cantilever, oscillating in the $x$ direction, is brought near a surface. A polarizing magnetic field is applied along the $y$ axis, in the direction of the cantilever width. Sample spins are inverted using a frequency-sweep adiabatic rapid passage (rf coil, not shown). (b) The inverted spins transiently shift the mechanical resonance frequency of the cantilever. (c) Cantilever frequency shift in GaAs at a temperature of 4.2 K. Spins are flipped at time $t=10$ s and again at $t=30$ s. Data from Ref. 154.

contours determined by the initial and final frequencies of the rapid passage. Subtracting the force gradient before and after the rapid passage results in a spring constant change given by

$$\Delta k_x = 2\sum_j \mu_{zj} \frac{\partial^2 B_z(\mathbf{r}_j)}{\partial x^2}, \tag{6}$$

where the sum is over the *inverted* spins in the sample. If the inverted region is chosen appropriately, $\partial^2 B_z/\partial x^2$ will be all one sign over the region. The resulting nonzero change in force gradient will shift the cantilever frequency by an amount $\Delta f_c \approx f_c \Delta k_x/2k$. If a large ensemble of spins is observed, an exponential recovery of the cantilever frequency should be seen while the longitudinal component of sample magnetization returns to equilibrium via spin lattice relaxation [Fig. 2(b)].

Garner *et al.* demonstrated the CERMIT effect by using it to detect magnetic resonance from $^{71}$Ga spins in a GaAs wafer at 4.2 K and at a field near 7 T using a custom-fabricated cantilever having a 9 $\mu$m diameter magnetic tip.[154] Representative signal is shown in Fig. 2(c). A shift in the cantilever frequency can be seen that is coincident with an adiabatic rapid passage applied at time $t=10$ s and again at $t=30$ s. The cantilever frequency shift is only seen when the static field is set to meet the magnetic resonance condition. This expected exponential recovery of cantilever frequency was too long to see in this experiment; the $^{71}$Ga spins studied had a $T_1$ of over 20 min. The long-term cantilever frequency drift seen in Ref. 154 suggests that spin-lattice relaxation times in the range of $T_1=0.01-100$ s should be observable in real time using CERMIT.

### B. Potential advantages of the CERMIT approach

The experiment of Garner *et al.* was the first reported example of magnet-on-cantilever NMR-MRFM—in other words, the first demonstration of *scanned probe* NMR. The experiment, moreover, showed that even a cantilever with a spring constant as low as 60 $\mu$N/m and a tip with a diameter as large as 9 $\mu$m could be operated at a field of 7 T. With the field oriented along the width of the cantilever [the $y$ axis of Fig. 2(a)], the frequency and quality factor of the magnetic-tipped cantilever remained essentially unperturbed by the high applied field and equal to their zero field values. The experiment of Ref. 154 was also noteworthy for its sensitivity: $\mu_{\min}=7.2\times10^{-21}$ J/T in a 1 Hz bandwidth—at the time of publication, the most sensitive demonstration of mechanically detected NMR yet published.

As can be seen from Fig. 2, both the CERMIT and the iOSCAR protocol are compatible with the most force sensitive cantilevers, which must be operated with their long axis normal to the surface. The CERMIT experiment, however, does not rely on a left-right statistical imbalance in spin polarization to create a signal; the CERMIT effect works naturally with Curie-law magnetization[154] as well as with statistical polarization.[50] A few other attributes of the CERMIT experiment set it apart from iOSCAR and force-based approaches. Additionally, the rf duty cycle is very low in the CERMIT experiment, a potentially huge advantage given that rf heating of the cantilever in low-temperature MRFM experiments is a major concern.[149,151]

Note also that, in Fig. 2(c), the signal lasts for over twenty seconds, much longer than any other mechanically detected spin signal to date. The detection bandwidth in the CERMIT experiment is potentially as narrow as $1/T_1$—much smaller and more favorable than the $\sim 1/T_{1\rho}$ detection bandwidth limit in previous methods to mechanical detection. In the experiment of Ref. 154, this possible signal-to-noise advantage was largely undone by surface noise. The CERMIT experiment, as described, is susceptible to signal-to-noise degradation by the $1/f$ fluctuations in cantilever frequency seen ubiquitously near surfaces in all MRFM experiments carried out to date.

The problem of surface noise has been addressed by Mamin *et al.* who introduced a cyclic-CERMIT experiment in which the cantilever frequency shift is modulated at 50 Hz by turning on the rf (and flipping the spins) every 20 ms for half a cantilever cycle.[50] The experiment of Ref. 50 confirms that the CERMIT approach dramatically reduces cantilever

heating and establishes that the effect can be used to detect statistical polarization. The coherence time of the spins in the cyclic-CERMIT experiment, however, was disappointingly low—much less than $T_1$ and more like $T_{1\rho}$. It should be noted, however, that the iOSCAR spin flips used to modulate magnetization in the Mamin *et al.* experiment are the most adiabatic off to each side of the cantilever instead of directly below the cantilever, where spins contribute most strongly to the CERMIT frequency shift. Further research is needed to ascertain whether the theoretical maximum coherence time of $T_1$ could be observed in a cyclic-CERMIT experiment by applying more nearly adiabatic spin flips. Despite these limitations, Mamin *et al.* used cyclic-CERMIT to demonstrate approximately 1200 fluorine nuclear spin sensitivity (for 10 min of averaging) and 90 nm imaging resolution.

If $1/f$ surface frequency noise can be tolerated, then the CERMIT effect could be used to monitor spin-lattice relaxation in a single-shot experiment, in real time—an exciting possibility given that $T_1$ measurements are extremely time consuming via inductive detection.

### C. Single-spin CERMIT

The magnet in the CERMIT experiment should be made as small as possible in order to produce the largest possible spring constant change per spin. This is problematic, because for Eq. (6) to remain valid, the cantilever amplitude must be kept much smaller than the distance from the center of the magnet (assumed spherical) to the sample surface. This is at odds with minimizing the noise in the cantilever frequency, which demands that the cantilever be driven to as large an amplitude as possible. To resolve this apparent paradox, in this section we present an extension to Eq. (6) that is valid for any cantilever amplitude. We will use this exact expression to consider the CERMIT signal in the single-spin limit.

The energy of the cantilever is given by

$$U = \tfrac{1}{2}m\dot{x}^2 + \tfrac{1}{2}kx^2 + V(x), \tag{7}$$

where $m$, $x$, and $k$ are cantilever mass, position, and spring constant, respectively. Here, $V(x)$ is the additional potential arising from the interaction of the cantilever's magnetic tip with the spins in the sample below. Consider a cantilever with its long axis directed along the $z$ direction, oscillating in the $x$ direction, and having a tip with radius $a$ and magnetization $\mathbf{M}=M\hat{z}$. Consider the interaction between this tip and a single spin having a magnetic moment $\boldsymbol{\mu}=\mu_z\hat{z}$ located at position $(0,0,z)$ relative to the center of the spherical tip. The relevant interaction potential, in SI units, depends on the displacement of the cantilever $x$ as follows:

$$V(x) = -\mu_z B_z = -\mu_z \frac{\mu_0 M a^3}{3}\frac{2z^2 - x^2}{(z^2+x^2)^{5/2}}. \tag{8}$$

We wish to derive an expression for how $V(x)$ perturbs the oscillator period. Toward this end, consider that when the cantilever position is at an extremum $x_m$, defined as the point where $\dot{x}=0$,

$$U = \tfrac{1}{2}kx_m^2 + V(x_m). \tag{9}$$

Equating Eqs. (7) and (9) and solving for $\dot{x}$, we have

$$\frac{dx}{dt} = \sqrt{\omega_0^2\left(x_m^2 - x^2 + \frac{2}{m}(V(x_m) - V(x))\right)}, \tag{10}$$

where we have used $k/m=\omega_0^2$. Now isolate time and position on separate sides of the equation and integrate each side over half a period (e.g., integrate $t$ from 0 to $T/2$ and $x$ from $-x_m$ to $+x_m$). In carrying out the integral, we will assume that the potential is a symmetric function of $x$, which is the case here. Solving for the period,

$$T = \frac{2}{\omega_0}\int_{-x_m}^{+x_m}\frac{dx}{\sqrt{x_m^2 - x^2 + \frac{2}{k}(V(x_m) - V(x))}}. \tag{11}$$

Define the cantilever period in the absence of the perturbation $V$ to be $T_0$. The shift in the cantilever period due to the perturbation is $\Delta T = T - T_0$. To first order in $1/k$, the shift is given by

$$\Delta T \approx -\frac{2}{\omega_0 k}\int_{-x_m}^{+x_m}\frac{V(x_m) - V(x)}{(x_m^2 - x^2)^{3/2}}dx. \tag{12}$$

The minimum detectable period shift may be derived from the minimum detectable spring constant shift $\Delta k_{\min} = S_F\sqrt{2b}/x_m$, which depends on the detection bandwidth $b$, the cantilever amplitude $x_m$, and spectral density $S_F$ of stochastic thermal forces acting on the cantilever. A small spring constant change will shift the cantilever frequency $f_0$ by an amount $\Delta f \approx f_0 \Delta k/2k_0$, where $k_0$ is the nascent cantilever spring constant. The resulting period shift is $\Delta T \approx -\Delta f/f_0^2$. From these considerations, it follows that $\Delta T_{\min} = S_F\sqrt{2b}/2k_0 f_0 x_m$. The signal-to-noise ratio for detecting the perturbation-induced change in cantilever period is $|\Delta T|/\Delta T_{\min}$,

$$\mathrm{SNR}_{\Delta T} = \frac{2}{S_F\pi\sqrt{2b}}x_m\int_{-x_m}^{+x_m}\frac{V(x_m) - V(x)}{(x_m^2 - x^2)^{3/2}}dx. \tag{13}$$

Substituting Eq. (8) into Eq. (13) gives an expression for the signal to noise ratio for detecting the period shift of a single spin using the CERMIT effect. This expression may be written in terms of the two unitless variables $\hat{x}\equiv x/x_m$ and $\hat{z}\equiv z/x_m$ as

$$\mathrm{SNR}_{\Delta T} = \frac{1}{S_F\sqrt{2b}}\frac{\mu_z\mu_0 M a^3}{z^4} \times \underbrace{\frac{2}{3\pi}\hat{z}^4\int_{-1}^{+1}\frac{d\hat{x}}{(1-\hat{x}^2)^{3/2}}\left\{\frac{1-2\hat{z}^2}{(1+\hat{z}^2)^{3/2}} - \frac{\hat{x}^2 - 2\hat{z}^2}{(\hat{x}^2+\hat{z}^2)^{3/2}}\right\}}_{I(\hat{z})}. \tag{14}$$

The underbraced term, $I(\hat{z})$, is unitless, and a function only of $\hat{z}$. Carrying out the integral numerically, we find that $I$ is a maximum $I(\hat{z}_m^{\max}) \approx 0.998$ at $\hat{z}_m^{\max} \approx 2.1$, or equivalently, when $x_m^{\max} \approx 0.47z$. Assuming we are oscillating the tip at this optimal amplitude,

$$\mathrm{SNR}_{\Delta T}^{\mathrm{CERMIT}} = \frac{1}{S_F\sqrt{2b}}\frac{1.00\mu_z\mu_0 M}{a}\left(\frac{a}{z}\right)^4. \tag{15}$$

The frequency shift in the OSCAR experiment is given by,[149,153] in our notation, $\Delta f = 2f_0 G\mu_z/\pi k_0 x_m$ with $G = \partial B_z/\partial x$. Converting this to an equivalent period shift for purposes of comparison, the signal-to-noise ratio for the OSCAR experiment is given by $\mathrm{SNR}_{\Delta T} = 4\mu_z G/\pi S_F\sqrt{2b}$. The gradient

$$G = \frac{\partial B_z}{\partial x} = \mu_0 M a^3 \left( \frac{x}{(x^2+z^2)^{5/2}} - \frac{5z^2 x}{(x^2+z^2)^{7/2}} \right) \tag{16}$$

is optimized for a spin located off to the side at $x \approx 0.389z$. The optimized gradient is $0.914\mu_0 M a^3/z^4$, with the result that

$$\mathrm{SNR}_{\Delta T}^{\mathrm{OSCAR}} = \frac{1}{S_F\sqrt{2b}} \frac{1.16\mu_z\mu_0 M}{a} \left(\frac{a}{z}\right)^4. \tag{17}$$

Comparing Eqs. (17) and (15), we can see that the signal-to-noise ratio for the single-spin OSCAR and optimal-amplitude single-spin CERMIT experiments depend identically on magnet diameter and height and are completely equivalent to within a small numerical factor.

## VI. UNDERSTANDING NONCONTACT FRICTION: SCAN PROBE DETECTION OF LOCAL ELECTRIC FIELD FLUCTUATIONS

Noise in inductively detected NMR is dominated by Johnson noise in the inductor. In MRFM, the main source of noise is thermomechanical position fluctuations in the mechanical oscillator. While the resistance in inductors is well understood, the analogous effect in cantilevers—damping—is poorly understood.

### A. Noncontact friction

Thermomechanical position and frequency fluctuations in an oscillator are governed by a fluctuation-dissipation relationship. The minimum force, and therefore force gradient, that a cantilever can detect is inextricably linked to the friction, or dissipation, that it experiences with the environment. The minimum detectable force is given by

$$F_{\mathrm{min}} = \sqrt{4\Gamma_t k_B T b}, \tag{18}$$

where $\Gamma_t$ is the total friction experienced by the cantilever, $k_B$ is Boltzmann's constant, $T$ is temperature, and $b$ is the bandwidth of the measurement. Cantilevers in MRFM experiments experience two types of friction: intrinsic friction $\Gamma_0$ and noncontact friction $\Gamma_s$ between the tip of the cantilever and the surface of the sample. These two contributions to the total cantilever friction add, $\Gamma_t = \Gamma_0 + \Gamma_s$. For the highest sensitivity force sensors $\Gamma_0 = k/\omega_0 Q$ has been minimized by fabricating cantilevers with small spring constants and high quality factors. Here, $k$, $\omega_0$, and $Q$ are the spring constant, resonance frequency, and quality factor, respectively, of the cantilever.

The attonewton-sensitivity cantilevers that allow MRFM to detect small numbers of spins push force microscopy into a previously unexplored regime where noncontact interactions between the cantilever tip and the sample dominate the measurement noise ($\Gamma_s > \Gamma_0$).[50,140,149,154] Understanding the mechanism of this noncontact interaction is critical to pushing MRFM toward single nuclear spin detection.

The friction that an underdamped classical oscillator experiences with its environment is set by the spectral density of the force fluctuations acting on the cantilever at its resonance frequency $[S_F(\omega_0)]$. Consequently, to elucidate the mechanism leading to increased $\Gamma_s$ is to discover the origin of force fluctuations acting on the cantilever due to the sample. In all MRFM experiments to date, surface friction has been found to depend quadratically on tip voltage (or, equivalently, tip charge). This finding immediately suggests that the fluctuating forces giving rise to cantilever dissipation originate from fluctuating electric fields in the sample,[155–157] with the result that

$$\Gamma_s = \frac{q^2 S_E(\omega_0)}{4k_B T}, \tag{19}$$

where $q$ is the charge on the tip, and

$$S_E(\omega_0) = 4\int_0^\infty \cos(\omega_0 t)\langle \delta E_x(t)\,\delta E_x(0)\rangle dt \tag{20}$$

is the electric field fluctuation spectral density at the cantilever's fundamental frequency arising from the sample.

Initial work, by Stipe *et al.*, directed towards understanding noncontact friction and force fluctuations using high sensitivity cantilevers measured dissipation using a metal-coated low-compliance cantilever over metal and quartz substrates at tip-sample separations down to 2 nm and temperatures from 4 to 300 K.[156] Friction over $\gamma$-irradiated quartz samples, of interest to electron spin MRFM experiments, was found to be orders of magnitude higher than that over metals. Noncontact friction was found to decrease with temperature by approximately a factor of 6 from 300 to 77 K and by another factor of 6 between liquid nitrogen temperature and 4 K. Most notably, friction over Au(111) was found to be seven orders of magnitude larger than predicted by Coulomb drag theories.[158]

In an effort to explain the anomalously high friction observed over metals, several theoretical proposals were set forth.[159–165] It was postulated by Volokitin and Persson that thermal fields could become resonant with modes in the surface, thereby promoting photon tunneling and thus dissipation between the cantilever and the surface.[166] This mechanism requires that the surface contain modes which are of low enough energy to be excited by thermal fields. This condition was said to be met by adsorbate vibrational transitions.[167] In the high vacuum experiments by Stipe *et al.*, surface adsorbates may have contributed to noncontact friction. As yet, no ultrahigh vacuum (UHV) experiments using high sensitivity cantilevers have corroborated this hypothesis.

Zurita–Sanchez *et al.* describe friction resulting from fluctuating thermal fields arising deep in the sample substrate.[162] They calculated that thermal fluctuations in the sample substrate could contribute significantly to the friction experienced by the oscillator. The authors concluded that the

large discrepancy between theory and experiment measured by Stipe *et al.* was due to the mica substrate on which the metal film was evaporated.

We undertook experiments using high sensitivity cantilevers to better understand the mechanisms of noncontact friction at play in high sensitivity force microscopy. Using low spring constant cantilevers operated in a geometry with their motion parallel to the sample surface, we studied the effects of dielectric layers on metal substrates. We demonstrated, for the first time, that dielectric fluctuations originating within the dielectric could enhance noncontact friction.[157] Our high vacuum measurements showed that noncontact friction, at room temperature, was strongly dependent on the chemical composition and the thickness of the dielectric layer. Further measurements showed no dependence of the friction over metal films on the substrate composition or metal layer thickness, results seemingly at odds with the predictions of Zurita–Sanchez *et al.* We were also able to show that adsorbed water on the surface of the sample was unlikely to be responsible for the large friction observed over metals.[157]

Our measurements were well described by a simple theoretical framework which used linear response theory and electrostatics to calculate the fluctuating field spectral density at the cantilever tip $[S_E(\omega_0)]$ due to dielectric fluctuations.[168] Using dielectric spectroscopy to independently measured dielectric properties of our samples, we were able to obtain a zero free parameter comparison between this theory and our measurements which fit the data exceptionally well. Further work is required to extend this theory to more general cases such as metals.

The need for further measurements of noncontact friction in the high sensitivity regime relevant to MRFM is critical. As yet, no definitive experiment has been done to elucidate the role of surface adsorbates in noncontact friction. A systematic study in a UHV apparatus would be poised to answer this pressing question. With the vast majority of MRFM experiments taking place in high vacuum, where surface adsorbates are certainly present, knowledge of the role of these adsorbates in measurement noise is necessary.

While noncontact friction deleteriously lowers the sensitivity of MRFM measurements, it can be exploited as a tool to image dopant density in semiconductors.[155,169] Harnessing the low intrinsic friction of our cantilevers to study local electric field fluctuations is a promising route to studying a number of materials. For example, imaging local charge diffusion in organic conductors might allow the local measurement of charge mobility—a long-sought goal that is simply impossible to reach using bulk measurements.

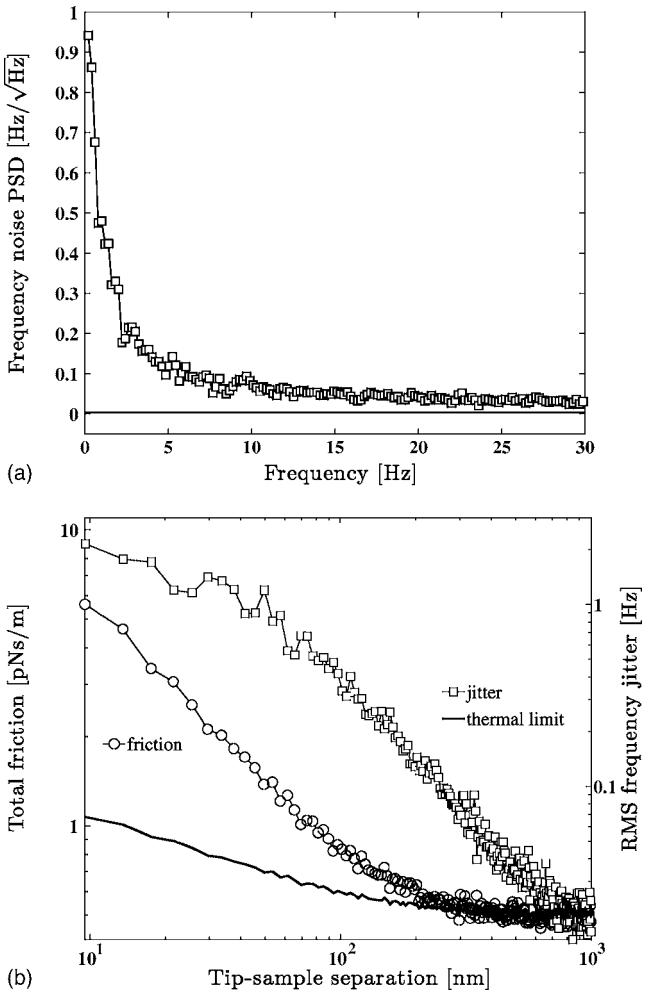


FIG. 3. (a) Frequency power spectrum for a cantilever at a height $h=114$ nm above a polystyrene film in high vacuum at $T=4$ K. The film of polystyrene (MW=143 000, PD≤1.09, Scientific Polymer Products) was 30 nm thick; it was spun from toluene onto a 200-nm-thick layer of Au that had been deposited at a rate of 0.05–0.1 nm/s via electron-beam evaporation onto a 20-nm-thick Cr adhesion layer on silicon. The single-crystal silicon cantilever was 340 nm thick and had a 1.0 $\mu$m wide leading edge. The cantilever, which was fabricated (Ref. 40) from a 14–22 $\Omega$ cm $p$-type ⟨100⟩-oriented silicon-on-insulator wafer, had parameters $k=100$ $\mu$N/m, $Q=1900$ (at $h=114$ nm), $f_c=2162$ Hz, an oscillation amplitude of $x_{\mathrm{rms}}=100$ nm, and was held a voltage of −5 V relative to the gold substrate. (b) Cantilever total friction ($\Gamma_t$; circles) and rms frequency jitter in a 10 Hz bandwidth near $f_c$ (squares) as a function of tip-sample separation over a 450-nm-thick poly(methyl-methacrylate) film (Ref. 157) at $T=300$ K. The cantilever parameters, oscillation amplitude, and tip potential were the same as in Ref. 157. For comparison, the solid line is the frequency jitter arising from thermomechanical position fluctuations of the cantilever, as calculated from the measured friction and the cantilever parameters and oscillation amplitude given in Ref. 157.

### B. Noise in frequency shift measurements

MRFM detection protocols such as OSCAR and CERMIT register the spin signal as a frequency shift in the cantilever.[125,154] In principle, these measurements should be subject to to the same noise limits as force detection schemes. In practice, however, low frequency force-gradient fluctuations drive the cantilever frequency fluctuations well above the thermal limit set by the cantilever friction.[170] Spurious force-gradient fluctuations lead to $1/f$ noise near $f_c$ in the cantilever frequency power spectrum.

This spurious $1/f$ noise can be seen in Fig. 3(a), in which we plot the frequency power spectrum of an ultrasensitive cantilever located 114 nm above a 30-nm-thick polystyrene film in high vacuum at $T=4$ K. The solid line is the frequency noise floor expected from thermal fluctuations $(0.0033\ \mathrm{Hz}/\sqrt{\mathrm{Hz}})$. At low frequency, the frequency noise is over ten times larger than this thermal limit.

To avoid the $1/f$ frequency noise, protocols such as iOS-

CAR and cyclic-CERMIT modulate the spin-dependent frequency shift coherently at a few tens of hertz.[50,140] While measurement noise is reduced using these schemes, thermally limited detection is typically not achieved. The origin of the force-gradient fluctuations which cause this excess frequency jitter remain unknown. For cantilevers in the perpendicular geometry, several mechanisms including cantilever deviations from perpendicularity and sample inhomogeneity must be considered.[171] The dominant mechanism of frequency fluctuations will depend on the tip-sample separation and tip size. As yet, careful experiments elucidating the dominant mechanism of cantilever frequency fluctuations in MRFM experiments have not been undertaken.

Low frequency noise in the cantilever frequency makes on-resonance force detection, in which modulated sample magnetization resonantly drives the cantilever and changes its oscillation amplitude, attractive. Despite this, on-resonance force detection places additional restrictions on the experiment by requiring long spin relaxation times and continuously applied rf. Experiments elucidating mechanisms of cantilever frequency noise at low frequency are therefore desirable.

## VII. FUTURE DIRECTIONS IN MECHANICALLY DETECTED MAGNETIC RESONANCE

The last decade of MRFM research has demonstrated that pushing sensitivity requires satisfying many competing constraints. For example, vibration isolation is at odds with heat sinking. Achieving long spin modulation times requires delivering large transverse rf magnetic fields, which is at odds with low-temperature experiments.

*Surface noise mitigation*. Achieving attonewton or subattonewton force sensitivity when the cantilever is operating near a surface would be a major breakthrough. Since a comprehensive understanding of surface-related dissipation mechanisms is not presently available and, moreover, will certainly be sample dependent, a general prescription for mitigating surface-related force noise cannot be given. Nevertheless, based on what is known already, a few promising avenues may be identified.

One approach to minimizing surface noise is to work with the sample on the cantilever. In this case, Mamin *et al.* have shown that surface noise can be substantially reduced by forming the magnetic tip into a sharp needle, which presumably limits the exposure of the cantilever to fluctuating electric fields in the substrate, while simultaneously metal coating the end of the cantilever to electrically screen the sample from laser-induced charge noise in the cantilever.[50]

Imaging technologically interesting samples most certainly requires working with the magnet on the cantilever. In this case, low-frequency electric field fluctuations in the sample can be screened by coating the sample with a thin metal overlayer.[157] However, in all high-vacuum magnet-on-cantilever MRFM experiments carried out to date, audio frequency cantilevers experience considerable surface friction even over gold. It is not clear whether the associated electric field fluctuations are intrinsic to the metal or are instead related to thermal motion of surface adsorbates. If surface dissipation in this case can be shown to be adsorbate related, then working in ultrahigh vacuum would be advantageous.

Another approach to mitigating surface noise is to work with radio frequency cantilevers. For nonconducting polymer samples, at least, one would expect the spectral density of electric field fluctuations to be much lower at megahertz frequencies than at kilohertz frequencies. Given this, the findings of Kuehn *et al.*[157,168] suggest that radio frequency cantilevers should experience significantly less surface dissipation over polymer (and, perhaps, biopolymer) samples than do audio frequency cantilevers.

Weitekamp *et al.* have proposed minimizing surface noise by placing the sample and magnet together on a torsional resonator.[172,173] The idea is that reorientation of spin magnetization at resonance can be used to apply a torque to the magnet-resonator assembly. Detecting the resulting rotation could be facilitated, by analogy with what is done in ion cyclotron resonance,[174] via parametrically exchanging rotational quanta and translational quanta. Extending this idea, Weitekamp *et al.* have suggested a route to eliminating even the elastic damping of the mechanical resonator—by levitating the sample-magnet assembly.

*Radio frequency field generation*. Poggio *et al.* have demonstrated that a 2.5 $\mu$m long, 1.0 $\mu$m wide, 0.2 $\mu$m thick copper microwire placed within 100 nm of the sample can deliver up to 4 mT of rf magnetic field using only 350 $\mu$W.[175] This strong rf field gave a huge $T_{1\rho}$ improvement in the $CaF_2$ sample studied. In their demonstration, Poggio *et al.* prepared a 200 nm FeCo magnet on the microwire; the sample was evaporated onto the cantilever. It is an open question whether biologically or technologically interesting samples can be affixed to an ultrasensitive cantilever. On the other hand, generating large rf fields at low power for magnet-on-cantilever NMR-MRFM studies of interesting samples remains a challenge as well.

Displacing the sample (in a sample-on-cantilever experiment) or the magnetic tip (in a magnet-on-cantilever experiment) at radio frequencies is a potentially very low power approach to creating large transverse magnetic fields. Using the motion of a rf cantilever to manipulate sample spin magnetization would obviate the need for an rf coil in the MRFM experiment and thereby facilitate operating the cantilever at millikelvin temperatures for greatly improved force sensitivity. Creating a distinguishable signature of magnetic resonance in a rf cantilever experiment may be challenging, however, since the motion of the cantilever and generation of the rf are not independent. New signal modulation schemes—perhaps based on parametric amplification[176,177] or second resonance[178]—will undoubtedly need to be developed. While a radio frequency cantilever has not yet, to our knowledge, been brought near a sample surface as in a scanned probe microscope experiment, we believe there is no reason that this milestone cannot be reached given the current state of the art.

*Displacement sensors*. Achieving thermally limited force detection of rf cantilever motion at cryogenic temperatures is extremely challenging, but has been achieved, for example, by coupling a rf single-electron transistor to a metal-coated $Si_3N_4$ cantilever[179] and by harnessing the piezoresistivity of

a thin metal film coating a SiC cantilever.[180] Displacement detectors based on tunnel sensors are under development for use with rf cantilevers,[181] and one can also imagine using on-chip ring resonators to achieve exquisitely sensitive displacement sensing.[182–184] Implementing rf cantilever displacement sensors in a MRFM experiment will demand carefully balancing the competing requirements of high displacement sensitivity and low force back action.

Sensitivity in all force-gradient MRFM experiments to date has been limited by noise in surface force gradients or by noise in the cantilever displacement detector. In audio frequency cantilever experiments that measure a time-dependent cantilever frequency, fast modulations [in order to avoid $1/f$ surface noise; see Fig. 3(a)] demand concomitantly large decreases in detector noise to achieve thermomechanical-force limited detection. To reach thermally limited sensitivity in a modulated-frequency MRFM experiment, much more sensitive displacement sensors will have to be developed.

*Cantilevers*. If surface noise can be mitigated, then developing cantilevers with improved sensitivity would be beneficial. The underlying sources of intrinsic cantilever dissipation remain under intense investigation both experimentally and theoretically.[185–194] Rast *et al.* have shown that annealing single crystal silicon cantilevers in ultrahigh vacuum can improve their mechanical quality factors by an order of magnitude.[195]

Nevertheless, achieving subattonewton sensitivity may require moving beyond single-crystal silicon oscillators. While $Si_3N_4$ was initially abandoned as a material for ultrasensitive cantilevers in favor of single crystal silicon,[38] recent work has shown that large increases in $Si_3N_4$'s mechanical quality factor can be realized by working at millikelvin temperature[179] or by applying strains.[196] Novel materials such as metallic glasses[197] may potentially exhibit ultralow mechanical dissipation. Nanocrystalline diamond[189,198] and carbon nanotube[199] cantilevers have recently been fabricated and appear to be promising force sensors.

*Spin modulation*. While both additional frequency fluctuations and loss of mechanical quality factor are seen near a surface, thermally limited amplitude fluctuations are maintained to a much closer tip-sample separation than are thermally limited frequency fluctuations. This effect can be see in Fig. 3(b), a plot of the total friction $\Gamma_t$ and the rms frequency jitter in a 10 Hz bandwidth as a function of height $h$ over a 450 nm thick poly(methyl-methacrylate) film at room temperature The friction is barely above the thermal limit at $h=200$ nm, whereas at $h=800$ nm, the jitter is already noticeably large. It is also apparent in the figure that at close approach the observed jitter is more than an order of magnitude larger than the expected frequency jitter arising from thermomechanical position fluctuations of the cantilever.

One route to avoiding the effect of surface-related force-gradient noise is to revert to force detection. Recall that force detection was abandoned in favor of iOSCAR because modulating the frequency of the applied rf (or the polarizing field) at the cantilever frequency, $f_c$ was found to excite the cantilever even in the absence of spin forces. Budakian *et al.* have recently shown how to modulate spin magnetization at $f_c$ with no feedthrough by using iOSCAR spins flips in conjugation with fast cantilever phase reversals.[170]

Here, we suggest an alternative approach to achieving force detection that should likewise avoid rf driving of the cantilever and, moreover, demands only a very low rf duty cycle. The basis for this approach is that spins below a cantilever oscillating parallel to the surface, as in Fig. 2(a), already present an oscillating force to a magnetic-tipped cantilever if the cantilever amplitude $x_c$ is large enough. Just below the tip, spins experience a time-dependent gradient $\partial B_z/\partial x \approx \partial^2 B_z/\partial x^2 \times x_c(t)$. If a time dependence can also be imposed on spin magnetization, then the spin below the tip will drive the cantilever with a force

$$F_x(t) = \mu_z(t)\frac{\partial^2 B_z}{\partial x^2}x_c(t). \tag{21}$$

If we turn on the rf once every $m$ cantilever cycles, as in the cyclic-CERMIT experiment, then this will modulate $\mu_z$ at a frequency $f_m=f_c/m$ which we might choose to be, say, 10 Hz. If the cantilever is driven below resonance at a frequency $f_x=f_c-f_m$, then, because the force depends on the product $\mu_z x_c$ which acts like a mixer, there will be a Fourier component in the force at $f_c$ that will resonantly excite the cantilever. We call this approach AM-cyclic-CERMIT, by analogy with the AM-iOSCAR approach of Budakian *et al.*[170]

*Magnetic particles*. It is important to note that the smallest diameter magnet does not necessarily give the largest signal-to-noise ratio. To see this, consider observing a spin located at a distance $h$ away from the surface of a cantilever's spherical magnetic tip. In this case, Eq. (15) becomes

$$\mathrm{SNR} = \frac{\mu_z \mu_0 M}{S_F(h)\sqrt{2b}}\frac{a^3}{(a+h)^4}, \tag{22}$$

where we have substituted $z=a+h$ and where we write $S_F(h)$ to emphasize that the minimum detectable force may depend on the tip-sample separation. If $h$ cannot be taken to zero experimentally, either because the target spin is buried or because force sensitivity degrades at small tip-sample separations, then a magnet radius of $a_{\mathrm{opt}}=3h_0$ optimizes the signal-to-noise ratio in a single spin MRFM experiment.[3]

In the single-electron ESR-MRFM experiment of Rugar *et al.*,[149] the tip magnet diameter was kept above a certain size in order to avoid dephasing sample spins from thermomagnetic fluctuations of tip magnetization. The comparatively low gyromagnetic ratio of protons makes them far less susceptible to tip-induced spin-lattice relaxation since $1/T_1 \propto \gamma^2$. We therefore do not expect spin dephasing of protons to be a problem as we decrease magnet size. Working at high field to damp tip magnetization fluctuations and create fully polarized magnetic tips is also technically much easier for protons than for electrons, because of the frequencies involved.

Because of concerns about beam-induced damage, fabricating the sub-50-nm diameter magnets needed to achieve single proton sensitivity will most certainly require eschewing focused ion beam milling and developing a lithographic fabrication route. Our studies of surface dissipation at 4 K

suggest that the magnets should overhang the leading edge of the cantilever to avoid compromising cantilever force sensitivity near surfaces. A number of groups have made progress in batch fabricating nanomagnets on ultrasensitive cantilevers,[40,41] although none have yet produced overhanging magnets. Nevertheless, initial work is promising. For example, the on-cantilever $1.2\times0.4\times0.2$ $\mu m^3$ nickel magnets of Jenkins *et al.*, patterned by electron beam lithography, had less than 30 nm of surface oxide and exhibited essentially bulk magnetization.[40]

*Imaging*. The established MRFM image-reconstruction protocols[47,69,70,74–76] have been designed to image Curie-law magnetization. With a sufficiently sharp tip and a thin planar sample, an image of small-ensemble magnetization fluctuations can be acquired directly by scanning, as the 90 nm resolution fluorine imaging experiment of Ref. 50 demonstrates. Nevertheless, considerable work needs to be done to understand signal-to-noise ratio and resolution in image reconstruction and image encoding in the small-ensemble limit. If near single-proton sensitivity and subangstrom resolution can be demonstrated, then we can imagine reaching a limit where sample spins become sparsely located and, if a biopolymer is studied, prior information or constraints on molecular structure may even be applied to aid in image reconstruction. Further work needs to be done to establish whether any advantage is obtainable by Fourier encoding[86] MRFM images in the single-spin or small-ensemble limits.

Optical pumping has already been used to increase MRFM signal in GaAs.[78,110] Applying dynamic nuclear polarization (DNP) to increase proton magnetization in organic samples is a potentially general approach to improving both imaging resolution and detection time in NMR-MRFM experiments. DNP efficiency in aqueous organic samples has shown dramatic improvement in recent years because techniques for generating high-power, very-high-frequency rf magnetic fields have advanced and because new biradical polarizing agents have been developed.[200] High frequency (94 GHz) irradiation has recently been employed in an ESR-MRFM experiment.[201]

The advantage of DNP in a MRFM experiment is that it would allow detection of a spin polarization with a well-defined sign. Consequently, averaging $N_{avg}$ signals would improve the power SNR by a factor of $N_{avg}$ [Eq. (3)] instead of the factor of $\sim\sqrt{N_{avg}}$ improvement attainable when observing polarization fluctuations [Eq. (4)].

The following example illustrates the potential benefit of DNP in a NMR-MRFM experiment. If detecting Boltzmann polarization, the relation between the minimum detectable magnetic moment $\mu_{min}$ and the minimal detectable volume of spins $V_{min}$ is $\rho V_{min}^{DNP}=\mu_{min}\mu_p^{-1}f^{-1}$ where $\rho$ is the proton density, $\mu_p$ is the proton magnetic moment, and $0<f<1$ is the fractional Boltzmann polarization achieved by DNP. If detecting polarization fluctuations, $\rho V_{min}^{fluct.}=\mu_{min}^2\mu_p^{-2}$. Suppose that $\mu_{min}=200\mu_p$ and $f=0.2$, $\rho V_{min}^{fluct.}=4\times10^4$, whereas $\rho V_{min}^{DNP}=1\times10^3$, a 40-fold improvement in the volume of spins that could be detected in single shot. A fairer comparison would account for the fact that the repetition time in the DNP experiment is limited by the polarization time $\tau_{DNP}$, whereas signal averaging can proceed much faster in the polarization-fluctuation experiment where the repetition time is the spin coherence time $\tau_m$ or faster. Suppose $\tau_{DNP}=60$ s and $\tau_m=1$ s. Then during DNP, $\mu_{min}$ in the polarization-fluctuation experiment would have improved by $\sqrt[4]{\tau_{DNP}/\tau_m}=2.78$ and the minimum detectable volume improved to $\rho V_{min}^{fluct.}=5\times10^3$, still a factor of 5 worse than that for $\rho V_{min}^{DNP}$ in this example.

*Theory*. As MRFM sensitivity improves to allow real-time single-spin detection, experiments will require a more sophisticated understanding of how quantum jumps of magnetization, wavefunction collapse, and back action might manifest themselves in a MRFM experiment.[202–208] Theorists have begun to treat the cantilever, spin, and interferometer in a MRFM experiment as quantum objects coupled to each other and to a thermal bath.[209–211] Theory is acutely needed to chart out how electron and nuclear spin magnetization might diffuse in large gradients.[212,213] Also, of pressing interest is Sidles' suggestion that saturating electron spins in strong gradients could lead to a new mechanism of dynamic nuclear polarization.[66]

## VIII. CONCLUSIONS

If it could be achieved in an MRFM experiment, detecting and imaging magnetic resonance from a single proton would represent both a new tool for determining protein structure and a general method for the interrogation of matter at the atomic scale. Such measurements would enable the elucidation of the atomic structure of small quantities of noncrystalline material, something which remains out of reach for all currently available analytical techniques. In addition, at single-nucleon sensitivity, MRFM could be exploited to explore fundamental quantum measurement processes. For example, MRFM could be used to readout the quantum state of single nuclear spin in a solid-state quantum computer. Nuclear spins remain attractive as quantum bits due to their generally long coherence times and the well established techniques for manipulating their quantum states.

While achieving single proton sensitivity by mechanical detection may seem like a far fetched goal, one must keep in mind that the smallest spin magnetic moment observable in a MRFM experiment has improved by a factor of $10^6$–$10^7$ since 1992. The first demonstration of MRFM achieved a magnetic moment sensitivity of $1.5\times10^{-17}$ J/T in an electron spin resonance experiment. By 2004, this sensitivity was improved to $1.9\times10^{-24}$ J/T for electron spin detection, and by 2007, to $1.6\times10^{-23}$ J/T for nuclear spin detection.

Ongoing efforts to mitigate surface noise, develop new spin-modulation schemes, fabricate nanoscale magnetic particles, and improve cantilever force sensitivity and readout at low temperatures suggest that MRFM sensitivity will continue to improve. We therefore believe that the prospects are excellent for detecting and imaging ESR at single-spin sensitivity in technologically interesting samples, such as a single copy of a nitroxide-labeled biomolecule. It is worth noting that the ultrasensitive cantilevers developed to improve MRFM sensitivity have, by themselves, enabled exciting breakthroughs in the measurement of fluctuations in single nanoparticle magnetization and in scan-probe charac-

terization of fluctuations in surface electric fields and electric field gradients. Independent of continuing advances in MRFM, such "spin-off" applications of ultrasensitive cantilevers hold great promise in materials characterization.

The primary interest in MRFM, however, remains the possibility of using the technique to obtain three dimensional imaging of the nuclear coordinates of a single copy of a frozen biomolecule. We have tried here to summarize the known impediments to further improving MRFM sensitivity and the work that is underway, in our laboratory and elsewhere, to overcome these impediments. As with developing other ultrasensitive magnetic resonance techniques, these breakthroughs will require devoting effort in research areas, such as cryogenic scanned probe microscopy and nanofabrication, that are far afield from traditional magnetic resonance. Single proton sensitivity, if it can be achieved, will likely require another tenfold improvement in cantilever sensitivity, further improvements in magnetic field gradients, and may well require application of a new generation of displacement sensors.

## ACKNOWLEDGMENTS

We gratefully acknowledge the support of the National Institutes of Health under Grant No. 5R01GM-070012 and the Army Research Office Multiuniversity Research Initiative under Grant No. W911NF-05-1-0403. This work was performed in part at the Cornell NanoScale Science and Technology Facility, a member of the National Nanotechnology Infrastructure Network, which is supported by the National Science Foundation through Grant No. ECS-0335765. S.K. acknowledges additional support from the Society of Analytical Chemists of Pittsburgh through the Analytical Division of the American Chemical Society.

We would like to acknowledge those colleagues of ours who attended the recent international workshop, "Magnetic Resonance Force Microscopy: Routes to Three-Dimensional Imaging of Single Molecules," held on June 21-24, 2006, at Cornell University. This workshop brought together over sixty researchers from the United States, Japan, Taiwan, Scotland, the Netherlands, Germany, Switzerland, and France, to assay progress and discuss future directions in MRFM. A list of participants and copies of many of the workshop's presentations are available at http://www.research.cornell.edu/KIC/ in the /events/MRFM2006/ subdirectory. While the conclusions in this paper are solely those of the authors, we have tried to document ideas expressed at the Kavli MRFM workshop in Sec. VII. The workshop was supported by grants from the Kavli Institute at Cornell for Nanoscale Science and the National Science Foundation Under Grant No. DMR-0634455, with additional funding from IBM, Eastman Kodak, and the New York State Office of Science, Technology, and Academic Research.

We particularly thank Dan Rugar for his insightful comments on an early draft of this manuscript. We acknowledge both Dan Rugar and Beat Meier for making their results available to us prior to publication.

[1] J. Sidles, Appl. Phys. Lett. **58**, 2854 (1991).
[2] J. Sidles, Phys. Rev. Lett. **68**, 1124 (1992).
[3] J. A. Sidles, J. L. Garbini, K. J. Bruland, D. Rugar, O. Züger, S. Hoen, and C. S. Yannoni, Rev. Mod. Phys. **67**, 249 (1995).
[4] See http://www.pdb.org for a database of known protein structures.
[5] See http://blanco.biomol.uci.edu for a database of known membrane protein structures.
[6] R. R. Ernst, B. Bodenhausen, and A. Wokaun, *Principles of Nuclear Magnetic Resonance in One and Two Dimensions* (Oxford University Press, New York, 1987).
[7] S. G. Zech, A. J. Wand, and A. E. McDermott, J. Am. Chem. Soc. **127**, 8618 (2005).
[8] D. Zhou, G. Shah, M. Cormos, C. Mullen, D. Sandoz, and C. Rienstra, J. Am. Chem. Soc. **129**, 11791 (2007).
[9] B. Wylie, L. Sperling, H. Frericks, G. Shah, W. Franks, and C. Rienstra, J. Am. Chem. Soc. **129**, 5318 (2007).
[10] N. A. Oyler and R. Tycko, J. Am. Chem. Soc. **126**, 4478 (2004).
[11] A. M. Wolters, D. A. Jayawickrama, and J. V. Sweedler, Curr. Opin. Chem. Biol. **6**, 711 (2002).
[12] D. L. Olson, T. L. Peck, A. G. Webb, R. L. Magin, and J. V. Sweedler, Science **270**, 1967 (1995).
[13] A. Abragam, *Principles of Nuclear Magnetism* (Oxford University Press, Oxford, 1961).
[14] Y. Manassen, R. J. Hamers, J. E. Demuth, and A. J. Castallano, Phys. Rev. Lett. **62**, 2531 (1989).
[15] Y. Manassen, I. Mukhopadhyay, and N. R. Rao, Phys. Rev. B **61**, 16223 (2000).
[16] C. Durkan and M. E. Welland, Appl. Phys. Lett. **80**, 458 (2002).
[17] P. Messina, M. Mannini, A. Caneschi, D. Gatteschi, L. Sorace, P. Sigalotti, C. Sandrin, S. Prato, P. Pittana, and Y. Manassen, J. Appl. Phys. **101**, 053916 (2007).
[18] A. I. Ekimov and V. I. Safarov, Semicond. Sci. Technol. **15**, 179 (1972).
[19] *Optical Orientation*, edited by F. Meier and P. Zacharchenya (Elsevier, Amsterdam, 1984).
[20] J. Köhler, J. A. J. M. Disselhorst, M. C. J. M. Donckers, E. J. J. Groenen, J. Schmidt, and W. E. Moerner, Nature (London) **363**, 242 (1993).
[21] J. Wrachtrup, C. von Borczyskowski, J. Bernard, M. Orrit, and R. Brown, Nature (London) **363**, 244 (1993).
[22] J. Köhler, A. C. Brouwer, E. J. Groenen, and J. Schmidt, Science **268**, 1457 (1995).
[23] J. A. Marohn, P. J. Carson, J. Y. Hwang, M. A. Miller, D. N. Shykind, and D. P. Weitekamp, Phys. Rev. Lett. **75**, 1364 (1995).
[24] R. Tycko and J. A. Reimer, J. Phys. Chem. **100**, 13240 (1996).
[25] A. Gruber, A. Drabenstedt, C. Tietz, L. Fleury, J. Wrachtrup, and C. von Borczyskowski, Science **276**, 2012 (1997).
[26] C. von Borczyskowski, J. Kohler, W. E. Moerner, M. Orrit, and J. Wrachtrup, Appl. Magn. Reson. **31**, 665 (2007).
[27] F. Jelezko, T. Gaebel, I. Popa, A. Gruber, and J. Wrachtrup, Phys. Rev. Lett. **92**, 076401 (2004).
[28] F. Jelezko, T. Gaebel, I. Popa, M. Domhan, A. Gruber, and J. Wrachtrup, Phys. Rev. Lett. **93**, 130501 (2004).
[29] S. Schuler, T. Speck, C. Tietz, J. Wrachtrup, and U. Seifert, Phys. Rev. Lett. **94**, 180602 (2005).
[30] T. Gaebel, M. Domhan, I. Popa, C. Wittmann, P. Neumann, F. Jelezko, J. R. Rabeau, N. Stavrias, A. D. Greentree, S. Prawer, J. Meijer, J. Twamley, P. R. Hemmer, and J. Wrachtrup, Nat. Phys. **2**, 408 (2006).
[31] C. Santori, P. Tamarat, P. Neumann, J. Wrachtrup, D. Fattal, R. G. Beausoleil, J. Rabeau, P. Olivero, A. D. Greentree, S. Prawer, F. Jelezko, and P. Hemmer, Phys. Rev. Lett. **97**, 247401 (2006).
[32] P. Tamarat, T. Gaebel, J. R. Rabeau, M. Khan, A. D. Greentree, H. Wilson, L. C. L. Hollenberg, S. Prawer, P. Hemmer, F. Jelezko, and J. Wrachtrup, Phys. Rev. Lett. **97**, 083002 (2006).
[33] C. Tietz, S. Schuler, T. Speck, U. Seifert, and J. Wrachtrup, Phys. Rev. Lett. **97**, 050602 (2006).
[34] C. I. Pakes, P. W. Josephs–Franks, R. P. Reed, S. G. Corner, and M. S. Colclough, IEEE Trans. Instrum. Meas. **50**, 310 (2001).
[35] M. B. Ketchen, D. D. Awschalom, W. J. Gallagher, A. W. Kleinsasser, R. L. Sandstrom, J. R. Rozen, and B. Bumble, IEEE Trans. Magn. **25**, 1212 (1989).
[36] D. Rugar, C. Yannoni, and J. A. Sidles, Nature (London) **360**, 563 (1992).
[37] D. Rugar, O. Züger, S. Hoen, C. S. Yannoni, H. M. Vieth, and R. D. Kendrick, Science **264**, 1560 (1994).
[38] T. D. Stowe, K. Yasumura, T. W. Kenny, D. Botkin, K. Wago, and D.

Rugar, Appl. Phys. Lett. **71**, 288 (1997).
[39] P. Streckeisen, S. Rast, C. Wattinger, E. Meyer, P. Vettiger, C. Gerber, and H. J. Guntherodt, Appl. Phys. A: Mater. Sci. Process. **A66**, S341 (1998).
[40] N. E. Jenkins, L. P. DeFlores, J. Allen, T. N. Ng, S. R. Garner, S. Kuehn, J. M. Dawlaty, and J. A. Marohn, J. Vac. Sci. Technol. B **22**, 909 (2004).
[41] M. D. Chabot, J. M. Moreland, L. Gao, S. H. Liou, and C. W. Miller, J. Microelectromech. Syst. **14**, 1118 (2005).
[42] D. W. Lee, J. H. Kang, U. Gysin, S. Rast, E. Meyer, M. Despont, and C. Gerber, J. Micromech. Microeng. **15**, 2179 (2005).
[43] S. Mouaziz, G. Boero, G. Moresi, C. Degen, Q. Lin, B. Meier, and J. Brugger, Microelectron. Eng. **83**, 1306 (2006).
[44] A. Schaff and W. S. Veeman, J. Magn. Reson. **126**, 200 (1997).
[45] N. Nestle, A. Schaff, and W. S. Veeman, Prog. Nucl. Magn. Reson. Spectrosc. **38**, 1 (2001).
[46] K. Wago, O. Zuger, R. Kendrick, C. S. Yannoni, and D. Rugar, J. Vac. Sci. Technol. B **14**, 1197 (1996).
[47] O. Züger, S. T. Hoen, C. S. Yannoni, and D. Rugar, J. Appl. Phys. **79**, 1881 (1996).
[48] K. Wago, D. Botkin, C. S. Yannoni, and D. Rugar, Appl. Phys. Lett. **72**, 2757 (1998).
[49] K. J. Bruland, W. M. Dougherty, J. L. Garbini, J. A. Sidles, and S. H. Chao, Appl. Phys. Lett. **73**, 3159 (1998).
[50] H. J. Mamin, M. Poggio, C. L. Degen, and D. Rugar, Nat. Nanotechnol. **2**, 301 (2007).
[51] K. J. Bruland, J. Krzystek, J. L. Garbini, and J. A. Sidles, Rev. Sci. Instrum. **66**, 2853 (1995).
[52] J. A. Marohn, R. Fainchtein, and D. D. Smith, J. Appl. Phys. **86**, 4619 (1999).
[53] W. M. Dougherty, K. J. Bruland, J. L. Garbini, and J. A. Sidles, Meas. Sci. Technol. **7**, 1733 (1996).
[54] J. Mertz, O. Marti, and J. Mlynek, Appl. Phys. Lett. **62**, 2344 (1993).
[55] J. L. Garbini, K. J. Bruland, W. M. Dougherty, and J. A. Sidles, J. Appl. Phys. **80**, 1951 (1996).
[56] K. J. Bruland, J. L. Garbini, W. M. Dougherty, and J. A. Sidles, J. Appl. Phys. **80**, 1959 (1996).
[57] K. J. Bruland, J. L. Garbini, W. M. Dougherty, and J. A. Sidles, J. Appl. Phys. **83**, 3972 (1998).
[58] C. L. Degen, U. Meier, Q. Lin, A. Hunkeler, and B. H. Meier, Rev. Sci. Instrum. **77**, 043707 (2006).
[59] Y. Obukhov, K. C. Fong, D. Daughton, and P. C. Hammel, J. Appl. Phys. **101**, 034315 (2007).
[60] D. de Roover, L. M. Porter, A. Emami–Naeni, J. A. Marohn, S. Kuehn, S. Garner, and D. D. Smith, in Proceedings of the Tenth NSTI Nanotech Conference, Santa Clara, CA, USA, 2007 (unpublished).
[61] T. E. Kriewall, J. L. Garbini, J. A. Sidles, and J. P. Jacky, Trans. ASME, J. Dyn. Syst. Meas. **128**, 577 (2006).
[62] T. R. Albrecht, P. Grütter, D. Horne, and D. Rugar, J. Appl. Phys. **69**, 668 (1991).
[63] Z. Zhang, P. C. Hammel, and G. J. Moore, Rev. Sci. Instrum. **67**, 3307 (1996).
[64] T. A. Barrett, C. R. Miers, H. A. Sommer, K. Mochizuki, and J. T. Markert, J. Appl. Phys. **83**, 6235 (1998).
[65] D. D. Smith, J. A. Marohn, and L. E. Harrell, Rev. Sci. Instrum. **72**, 2080 (2001).
[66] W. M. Dougherty, K. J. Bruland, S. H. Chao, J. L. Garbini, S. E. Jensen, and J. A. Sidles, J. Magn. Reson. **143**, 106 (2000).
[67] R. Verhagen, C. W. Hilbers, A. P. M. Kentgens, L. Lenci, R. Groeneveld, A. Wittli, and H. van Kempen, Phys. Chem. Chem. Phys. **1**, 4025 (1999).
[68] K. J. Bruland, J. L. Garbini, W. M. Dougherty, S. H. Chao, S. E. Jensen, and J. A. Sidles, Rev. Sci. Instrum. **70**, 3542 (1999).
[69] O. Züger and D. Rugar, Appl. Phys. Lett. **63**, 2496 (1993).
[70] O. Züger and D. Rugar, J. Appl. Phys. **75**, 6211 (1994).
[71] P. Hammel, Z. Zhang, G. J. Moore, and M. L. Roukes, J. Low Temp. Phys. **101**, 59 (1995).
[72] Z. Zhang, M. L. Roukes, and P. C. Hammel, J. Appl. Phys. **80**, 6931 (1996).
[73] A. Suter, D. V. Pelekhov, M. L. Roukes, and P. C. Hammel, J. Magn. Reson. **154**, 210 (2002).
[74] S. Tsuji, T. Masumizu, and Y. Yoshinari, J. Magn. Reson. **167**, 211 (2004).
[75] S. H. Chao, W. M. Dougherty, J. L. Garbini, and J. A. Sidles, Rev. Sci. Instrum. **75**, 1175 (2004).
[76] S. Tsuji, Y. Yoshinari, H. S. Park, and D. Shindo, J. Magn. Reson. **178**, 325 (2006).
[77] S. H. Chao, J. L. Garbini, W. M. Dougherty, and J. A. Sidles, Rev. Sci. Instrum. **77**, 063710 (2006).
[78] K. R. Thurber, L. E. Harrell, and D. D. Smith, J. Magn. Reson. **162**, 336 (2003).
[79] K. W. Eberhardt, C. L. Degen, and B. H. Meier, Phys. Rev. B **76**, 180405 (2007).
[80] M. Barbic, J. Appl. Phys. **91**, 9987 (2002).
[81] M. Barbic and A. Scherer, J. Appl. Phys. **92**, 7345 (2002).
[82] M. Barbic and A. Scherer, J. Appl. Phys. **95**, 3598 (2004).
[83] M. Barbic and A. Scherer, J. Magn. Reson. **181**, 223 (2006).
[84] M. Barbic and A. Scherer, Nano Lett. **5**, 787 (2005).
[85] P. Brunner and R. R. Ernst, J. Magn. Reson. (1969-1992) **33**, 83 (1979).
[86] J. G. Kempf and J. A. Marohn, Phys. Rev. Lett. **90**, 087601 (2003).
[87] A. Kumar, D. Welti, and R. R. Ernst, J. Magn. Reson. (1969-1992) **18**, 69 (1975).
[88] P. Mansfield and P. G. Morris, *NMR Imaging in Biomedicine* (Academic, New York, 1982).
[89] E. Kupce and R. Freeman, Concepts Magn. Reson., Part A **22**, 4 (2004).
[90] E. Kupce and R. Freeman, J. Am. Chem. Soc. **126**, 6429 (2004).
[91] Z. Zhang, P. C. Hammel, and P. E. Wigen, Appl. Phys. Lett. **68**, 2005 (1996).
[92] B. J. Suh, P. C. Hammel, Z. Zhang, M. M. Midzor, M. L. Roukes, and J. R. Childress, J. Vac. Sci. Technol. B **16**, 2275 (1998).
[93] Z. Zhang, P. C. Hammel, M. Midzor, M. L. Roukes, and J. R. Childress, Appl. Phys. Lett. **73**, 2036 (1998).
[94] V. Charbois, V. V. Naletov, J. Ben Youssef, and O. Klein, J. Appl. Phys. **91**, 7337 (2002).
[95] V. Charbois, V. V. Naletov, J. Ben Youssef, and O. Klein, Appl. Phys. Lett. **80**, 4795 (2002).
[96] V. V. Naletov, V. Charbois, O. Klein, and C. Fermon, Appl. Phys. Lett. **83**, 3132 (2003).
[97] O. Klein, V. Charbois, V. V. Naletov, and C. Fermon, Phys. Rev. B **67**, 220407 (2003).
[98] O. Klein, V. Charbois, V. V. Naletov, and C. Fermon, J. Magn. Magn. Mater. **272**, E1027 (2004).
[99] O. Klein and V. V. Naletov, C. R. Phys. **5**, 325 (2004).
[100] G. de Loubens, V. V. Naletov, and O. Klein, Phys. Rev. B **71**, 180411 (2005).
[101] T. Mewes, J. Kim, D. V. Pelekhov, G. N. Kakazei, P. E. Wigen, S. Batra, and P. C. Hammel, Phys. Rev. B **74**, 144424 (2006).
[102] G. de Loubens, V. V. Naletov, O. Klein, J. Ben Youssef, F. Boust, and N. Vukadinovic, Phys. Rev. Lett. **98**, 127601 (2007).
[103] V. V. Naletov, G. de Loubens, V. Charbois, O. Klein, V. S. Tiberkevich, and A. N. Slavin, Phys. Rev. B **75**, 140405 (2007).
[104] E. Nazaretski, I. Martin, R. Movshovich, D. V. Pelekhov, P. C. Hammel, M. Zalalutdinov, J. W. Baldwin, B. Houston, and T. Mewes, Appl. Phys. Lett. **90**, 234105 (2007).
[105] M. Löhndorf, J. Moreland, and P. Kabos, Appl. Phys. Lett. **76**, 1176 (2000).
[106] R. Urban, A. Putilin, P. E. Wigen, S. H. Liou, M. C. Cross, P. C. Hammel, and M. L. Roukes, Phys. Rev. B **73**, 212410 (2006).
[107] E. Nazaretski, J. D. Thompson, R. Movshovich, M. Zalalutdinov, J. W. Baldwin, B. Houston, T. Mewes, D. V. Pelekhov, P. Wigen, and P. C. Hammel, J. Appl. Phys. **101**, 074905 (2007).
[108] T. G. Ruskell, M. Löhndorf, and J. Moreland, J. Appl. Phys. **86**, 664 (1999).
[109] A. Jander, J. Moreland, and P. Kabos, J. Appl. Phys. **89**, 7086 (2001).
[110] K. R. Thurber, L. E. Harrell, R. Fainchtein, and D. D. Smith, Appl. Phys. Lett. **80**, 1794 (2002).
[111] Y. J. Wang, M. Eardley, S. Knappe, J. Moreland, L. Hollberg, and J. Kitching, Phys. Rev. Lett. **97**, 227602 (2006).
[112] G. P. Berman, G. D. Doolen, P. C. Hammel, and V. I. Tsifrinovich, Phys. Rev. B **61**, 14694 (2000).
[113] G. P. Berman, G. D. Doolen, P. C. Hammel, and V. I. Tsifrinovich, Phys. Rev. Lett. **86**, 2894 (2001).
[114] G. P. Berman, F. Borgonovi, G. Chapline, P. C. Hammel, and V. I. Tsifrinovich, Phys. Rev. A **66**, 032106 (2002).
[115] K. Wago, O. Zuger, J. Wegener, R. Kendrick, C. S. Yannoni, and D. Rugar, Rev. Sci. Instrum. **68**, 1823 (1997).
[116] K. Wago, D. Botkin, C. S. Yannoni, and D. Rugar, Phys. Rev. B **57**, 1108 (1998).
[117] R. Verhagen, A. Wittlin, C. W. Hilbers, H. van Kempen, and A. P. M. Kentgens, J. Am. Chem. Soc. **124**, 1588 (2002).

[118] C. L. Degen, Q. Lin, A. Hunkeler, U. Meier, M. Tomaselli, and B. H. Meier, Phys. Rev. Lett. **94**, 207601 (2005).
[119] C. L. Degen, Q. Lin, and B. H. Meier, Phys. Rev. B **74**, 104414 (2006).
[120] Q. Lin, C. L. Degen, M. Tomaselli, A. Hunkeler, U. Meier, and B. H. Meier, Phys. Rev. Lett. **96**, 137604 (2006).
[121] K. W. Eberhardt, Q. Lin, U. Meier, A. Hunkeler, and B. H. Meier, Phys. Rev. B **75**, 184430 (2007).
[122] G. M. Leskowitz, L. A. Madsen, and D. P. Weitekamp, Solid State Nucl. Magn. Reson. **11**, 73 (1998).
[123] L. A. Madsen, G. M. Leskowitz, and D. P. Weitekamp, Proc. Natl. Acad. Sci. U.S.A. **101**, 12804 (2004).
[124] H. Bergh and E. W. McFarland, Meas. Sci. Technol. **7**, 1019 (1996).
[125] B. C. Stipe, H. J. Mamin, C. S. Yannoni, T. D. Stowe, T. W. Kenny, and D. Rugar, Phys. Rev. Lett. **87**, 277602 (2001).
[126] R. Budakian, H. J. Mamin, and D. Rugar, Phys. Rev. Lett. **92**, 037205 (2004).
[127] G. P. Berman, B. M. Chernobrod, V. N. Gorshkov, and V. I. Tsifrinovich, Phys. Rev. B **71**, 184409 (2005).
[128] K. W. Eberhardt, S. Mouaziz, G. Boero, J. Brugger, and B. H. Meier, Phys. Rev. Lett. **99**, 227603 (2007).
[129] D. Weitekamp, U.S. Patent No. 6,841,995 (January 11, 2005).
[130] I. Bargatin and M. L. Roukes, Phys. Rev. Lett. **91**, 138302 (2003).
[131] Z. Zhang and P. C. Hammel, IEEE Trans. Magn. **33**, 4047 (1997).
[132] Z. Zhang and P. C. Hammel, Solid State Nucl. Magn. Reson. **11**, 65 (1998).
[133] J. A. Marohn, R. Fainchtein, and D. D. Smith, Appl. Phys. Lett. **73**, 3778 (1998).
[134] B. C. Stipe, H. J. Mamin, T. D. Stowe, T. W. Kenny, and D. Rugar, Phys. Rev. Lett. **86**, 2874 (2001).
[135] C. W. Miller, U. M. Mirsaidov, T. C. Messina, Y. J. Lee, and J. T. Markert, J. Appl. Phys. **93**, 6572 (2003).
[136] T. N. Ng, N. E. Jenkins, and J. A. Marohn, IEEE Trans. Magn. **42**, 378 (2006).
[137] J. D. Hannay, R. W. Chantrell, and D. Rugar, J. Appl. Phys. **87**, 6827 (2000).
[138] D. Mozyrsky, I. Martin, D. Pelekhov, and P. C. Hammel, Appl. Phys. Lett. **82**, 1278 (2003).
[139] G. P. Berman, V. N. Gorshkov, D. Rugar, and V. I. Tsifrinovich, Phys. Rev. B **68**, 094402 (2003).
[140] H. J. Mamin, R. Budakian, B. W. Chui, and D. Rugar, Phys. Rev. Lett. **91**, 207604 (2003).
[141] G. P. Berman, V. N. Gorshkov, and V. I. Tsifrinovich, Phys. Rev. B **69**, 212408 (2004).
[142] G. P. Berman, V. N. Gorshkov, and V. I. Tsifrinovich, Phys. Lett. A **318**, 584 (2003).
[143] R. Budakian, H. J. Mamin, B. W. Chui, and D. Rugar, Science **307**, 408 (2005).
[144] H. J. Mamin, R. Budakian, B. W. Chui, and D. Rugar, Phys. Rev. B **72**, 024413 (2005).
[145] P. L. Carson, M. L., G. M. Leskowitz, and D. P. Weitekamp, Bull. Am. Phys. Soc. **44**, 541 (1999).
[146] P. L. Carson, M. L., G. M. Leskowitz, and D. P. Weitekamp, U.S. Patent No. 6,081,119 (June 27, 2000).
[147] E. Kreyszig, *Introductory Mathematical Statistics: Principles and Methods* (Wiley, New York, 1970).
[148] C. L. Degen, M. Poggio, H. J. Mamin, and D. Rugar, "The role of spin noise in the detection of nanoscale ensembles of nuclear spins," Phys. Rev. Lett. (in press).
[149] D. Rugar, R. Budakian, H. J. Mamin, and B. W. Chui, Nature (London) **430**, 329 (2004).
[150] H. J. Mamin and D. Rugar, Appl. Phys. Lett. **79**, 3358 (2001).
[151] H. J. Mamin, R. Budakian, and D. Rugar, Rev. Sci. Instrum. **74**, 2749 (2003).
[152] G. P. Berman, D. I. Kamenev, and V. I. Tsifrinovich, Phys. Rev. A **66**, 023405 (2002).
[153] G. P. Berman, F. Borgonovi, and V. I. Tsifrinovich, Phys. Rev. B **72**, 224406 (2005).
[154] S. R. Garner, S. Kuehn, J. M. Dawlaty, N. E. Jenkins, and J. A. Marohn, Appl. Phys. Lett. **84**, 5091 (2004).
[155] W. Denk and D. Pohl, Appl. Phys. Lett. **59**, 2171 (1991).
[156] B. C. Stipe, H. J. Mamin, T. D. Stowe, T. W. Kenny, and D. Rugar, Phys. Rev. Lett. **87**, 096801 (2001).
[157] S. Kuehn, R. F. Loring, and J. A. Marohn, Phys. Rev. Lett. **96**, 156103 (2006).
[158] B. J. Persson and Z. Zhang, Phys. Rev. B **57**, 7327 (1998).
[159] A. I. Volokitin and N. J. Persson, Phys. Rev. B **65**, 115419 (2002).
[160] A. I. Volokitin and B. N. J. Persson, Phys. Rev. B **68**, 155420 (2003).
[161] V. Mkrtchian, V. A. Parsegian, R. Podgornik, and W. M. Saslow, Phys. Rev. Lett. **91**, 220801 (2003).
[162] J. R. Zurita–Sanchez, J. J. Greffet, and L. Novotny, Phys. Rev. A **69**, 022902 (2004).
[163] A. I. Volokitin and B. N. J. Persson, Phys. Rev. B **74**, 205413 (2006).
[164] A. I. Volokitin, B. N. J. Persson, and H. Ueba, Phys. Rev. B **73**, 165423 (2006).
[165] A. I. Volokitin, B. N. J. Persson, and H. Ueba, J. Exp. Theor. Phys. **104**, 96 (2007).
[166] A. I. Volokitin and B. N. J. Persson, Phys. Rev. Lett. **91**, 106101 (2003).
[167] A. I. Volokitin and B. N. J. Persson, Phys. Rev. Lett. **94**, 086104 (2005).
[168] S. Kuehn, J. A. Marohn, and R. F. Loring, J. Phys. Chem. B **110**, 14525 (2006).
[169] T. D. Stowe, T. W. Kenny, D. J. Thomson, and D. Rugar, Appl. Phys. Lett. **75**, 2785 (1999).
[170] R. Budakian, H. J. Mamin, and D. Rugar, Appl. Phys. Lett. **89**, 113113 (2006).
[171] T. D. Stowe, Ph.D. thesis, Stanford University, 2000.
[172] M. Butler, R. Elgammal, V. A. Norton, and D. Weitekamp, Abstr. Pap. - Am. Chem. Soc. **227**, U328 (2004).
[173] M. Butler, V. Norton, and D. Weitekamp, Abstr. Pap. - Am. Chem. Soc. **229**, U735 (2005).
[174] E. A. Cornell, R. M. Weisskoff, K. R. Boyce, and D. E. Pritchard, Phys. Rev. A **41**, 312 (1990).
[175] M. Poggio, C. L. Degen, C. T. Rettner, H. J. Mamin, and D. Rugar, Appl. Phys. Lett. **90**, 263111 (2007).
[176] D. Rugar and P. Grütter, Phys. Rev. Lett. **67**, 699 (1991).
[177] M. Zalalutdinov, A. Olkhovets, A. Zehnder, B. Ilic, D. Czaplewski, H. G. Craighead, and J. M. Parpia, Appl. Phys. Lett. **78**, 3142 (2001).
[178] N. Tabuchi and H. Hatanaka, J. Magn. Reson. **148**, 121 (2001).
[179] A. Naik, O. Buu, M. D. LaHaye, A. D. Armour, A. A. Clerk, M. P. Blencowe, and K. C. Schwab, Nature (London) **443**, 193 (2006).
[180] M. Li, H. X. Tang, and M. L. Roukes, Nat. Nanotechnol. **2**, 114 (2007).
[181] N. E. Flowers–Jacobs, D. R. Schmidt, and K. W. Lehnert, Phys. Rev. Lett. **98**, 096804 (2007).
[182] V. R. Almeida, C. A. Barrios, R. R. Panepucci, and M. Lipson, Nature (London) **431**, 1081 (2004).
[183] Q. F. Xu, B. Schmidt, S. Pradhan, and M. Lipson, Nature (London) **435**, 325 (2005).
[184] M. Hossein–Zadeh and K. J. Vahala, Opt. Express **15**, 166 (2007).
[185] K. Y. Yasumura, T. D. Stowe, E. M. Chow, T. Pfafman, T. W. Kenny, B. C. Stipe, and D. Rugar, J. Microelectromech. Syst. **9**, 117 (2000).
[186] J. L. Yang, T. Ono, and M. Esashi, J. Microelectromech. Syst. **11**, 775 (2002).
[187] D. F. Wang, T. Ono, and M. Esashi, Appl. Phys. Lett. **83**, 3189 (2003).
[188] U. Gysin, S. Rast, P. Ruff, E. Meyer, D. W. Lee, P. Vettiger, and C. Gerber, Phys. Rev. B **69**, 045403 (2004).
[189] A. B. Hutchinson, P. A. Truitt, K. C. Schwab, L. Sekaric, J. M. Parpia, H. G. Craighead, and J. E. Butler, Appl. Phys. Lett. **84**, 972 (2004).
[190] Y. Wang, J. A. Henry, D. Sengupta, and M. A. Hines, Appl. Phys. Lett. **85**, 5736 (2004).
[191] T. Ono and M. Esashi, Appl. Phys. Lett. **87**, 044105 (2005).
[192] G. Zolfagharkhani, A. Gaidarzhy, S. B. Shim, R. L. Badzey, and P. Mohanty, Phys. Rev. B **72**, 224101 (2005).
[193] J. A. Henry, Y. Wang, D. Sengupta, and M. A. Hines, J. Phys. Chem. B **111**, 88 (2007).
[194] B. Lee and R. E. Rudd, Phys. Rev. B **75**, 195328 (2007).
[195] S. Rast, U. Gysin, P. Ruff, C. Gerber, E. Meyer, and D. W. Lee, Nanotechnology **17**, S189 (2006).
[196] S. S. Verbridge, D. F. Shapiro, H. G. Craighead, and J. M. Parpia, Nano Lett. **7**, 1728 (2007).
[197] A. L. Greer and E. Ma, MRS Bull. **32**, 611 (2007).
[198] L. Sekaric, J. M. Parpia, H. G. Craighead, T. Feygelson, B. H. Houston, and J. E. Butler, Appl. Phys. Lett. **81**, 4455 (2002).
[199] V. Sazonova, Y. Yaish, H. Ustunel, D. Roundy, T. A. Arias, and P. L. McEuen, Nature (London) **431**, 284 (2004).
[200] C. S. Song, K. N. Hu, C. G. Joo, T. M. Swager, and R. G. Griffin, J. Am. Chem. Soc. **128**, 11385 (2006).
[201] P. A. S. Cruickshank and G. M. Smith, Rev. Sci. Instrum. **78**, 015101 (2007).
[202] G. P. Berman and V. I. Tsifrinovich, Phys. Rev. B **61**, 3524 (2000).

[203] G. P. Berman, G. D. Doolen, P. C. Hammel, and V. I. Tsifrinovich, Phys. Rev. A **65**, 032311 (2002).
[204] G. P. Berman, F. Borgonovi, G. Chapline, S. A. Gurvitz, P. C. Hammel, D. V. Pelekhov, A. Suter, and V. I. Tsifrinovich, J. Phys. A **36**, 4417 (2003).
[205] G. P. Berman, F. Borgonovi, G. V. Lopez, and V. I. Tsifrinovich, Phys. Rev. A **68**, 012102 (2003).
[206] T. A. Brun and H. S. Goan, Phys. Rev. A **68**, 032301 (2003).
[207] G. P. Berman, F. Borgonovi, and V. Tsifrinovich, Phys. Lett. A **331**, 187 (2004).
[208] G. P. Berman, F. Borgonovi, and V. I. Tsifrinovich, Phys. Lett. A **337**, 161 (2005).
[209] H. Gassmann, M. S. Choi, H. Yi, and C. Bruder, Phys. Rev. B **69**, 115419 (2004).
[210] S. Mancini, D. Vitali, and H. Moya–Cessa, Phys. Rev. B **71**, 054406 (2005).
[211] T. A. Brun and H. S. Goan, Int. J. Quantum Inf. **3**, 1 (2005).
[212] A. G. Redfield, Phys. Rev. **116**, 315 (1959).
[213] A. Z. Genack and A. G. Redfield, Phys. Rev. B **12**, 78 (1975).